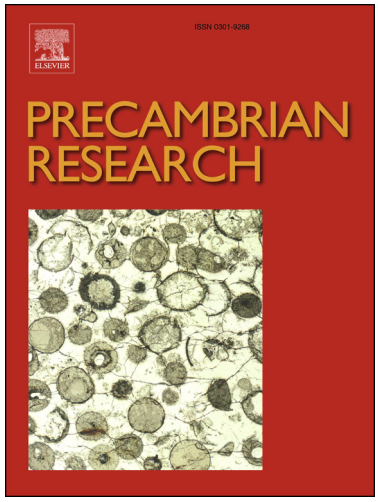

Global species richness record and biostratigraphic potential of early to middle Neoproterozoic eukaryote fossils

Leigh Anne Riedman, Peter M. Sadler

PII: S0301-9268(17)30253-X
DOI: https://doi.org/10.1016/j.precamres.2017.10.008
Reference: PRECAM 4906

To appear in: *Precambrian Research*

Received Date: 10 May 2017
Revised Date: 13 September 2017
Accepted Date: 5 October 2017

Please cite this article as: L.A. Riedman, P.M. Sadler, Global species richness record and biostratigraphic potential of early to middle Neoproterozoic eukaryote fossils, *Precambrian Research* (2017), doi: https://doi.org/10.1016/j.precamres.2017.10.008

Global species richness record and biostratigraphic potential of early to middle Neoproterozoic eukaryote fossils

Leigh Anne Riedman [a*] and Peter M. Sadler[b]

[a] Department of Earth and Planetary Sciences, Harvard University, Cambridge, MA 02138 USA
[b] Department of Earth Sciences, University of California, Riverside, Riverside, CA 92521, USA, peter.sadler@ucr.edu
*_Corresponding author_: lriedman@fas.harvard.edu, lariedman@gmail.com

Abstract

Over the past several decades, a number of studies have addressed the record of eukaryotic species richness in the Proterozoic, each making quite clear that during the Neoproterozoic Era, in particular, tremendous changes occurred in Earth's biota. The relative scarcity of radiometric age constraints for rocks of this interval, however, have necessitated the use of coarse time bins (~100 Ma) and the omission of fossiliferous but poorly dated units, resulting in low resolution of eukaryotic richness trends. Here we present a new estimate of early to middle Neoproterozoic (Tonian and Cryogenian) eukaryotic richness developed by use of the CONOP seriation algorithm; this approach permits inclusion of poorly dated and un-dated units and allows for greater resolution.

The CONOP (*con*strained *op*timization) algorithm operates by evolutionary ordination—considering evidence of stratigraphic order from all locations simultaneously and starting from a random ordinal sequence that improves by mutations retained or removed according to best-fit rules. This program has been applied successfully to biochronologic and biostratigraphic problems throughout the Phanerozoic geologic record. Here we apply this objective approach to a new compilation of taxonomically well-constrained organic-walled microfossil occurrences as well as geochemical, sedimentological and geochronological data from more than 160 formations from 60 groups in paleogeographically distant successions. From this dataset was developed a high-resolution eukaryotic species richness record for the early to middle Neoproterozoic Era (~1000 to 635 Ma).

This new estimate of eukaryotic species richness indicates an increase in richness began ~800 Ma and continued towards a peak ~770 Ma when it declined with the losses of many long-lived acritarch taxa. The overall decline is punctuated by a sharp richness increase with a ~738 Ma peak due to the iconic and short-lived Tonian vase-shaped microfossil taxa such as *Cycliocyrillium simplex*. These VSM taxa were lost ~733 Ma and richness continued to decline until flat-lining well in advance of the ~720 Ma onset of the Cryogenian Snowball Earth glaciations. Eukaryotic species richness did not rebound until after the termination of the second Cryogenian glaciation when a new suite of acritarch taxa appeared in the Ediacaran Period.

Use of CONOP with this dataset also permitted assessment of fossil taxa that had previously been suggested as Neoproterozoic biostratigraphic index taxa. Our results provide particular support for biostratigraphic use of the acritarch *Cerebrosphaera globosa* (=*C. buickii*) and for species of vase-shaped microfossils.

Keywords: Neoproterozoic, diversity, acritarch, Snowball Earth, *Cerebrosphaera*, Vase-shaped microfossils

1. Introduction

1.1 Neoproterozoic Eukaryote Species Richness

Paleontological as well as molecular clock data indicate that the early to middle Neoproterozoic Era was a time of major eukaryotic diversifications and extinctions (Knoll, 1994; Huntley et al., 2006; Knoll et al., 2006; Xiao and Dong, 2006; Parfrey et al., 2011; Riedman et al., 2014), the rise of eukaryote predation upon eukaryotes (Porter, 2011; Knoll and Lahr, 2015; Porter, 2016) and biomineralization (Porter and Knoll, 2000; Cohen et al., 2011). This interval was also marked by fluctuations in oceanic and atmospheric chemistry (Meyer and Kump, 2008; Canfield, 2014), formation and rifting of the supercontinent Rodinia (Li et al., 2008), major perturbations in the carbon cycle and at least two global glaciations (Snowball Earth events; Hoffman and Li, 2009). Understanding causal relationships between these biotic and abiotic events is a primary goal in Precambrian studies, but first a detailed timeline of broad-scale biological trends including eukaryotic diversifications and extinctions is necessary.

Over the past few decades several estimates of Precambrian eukaryotic richness and disparity have been published (Knoll, 1994; Vidal and Moczydłowska-Vidal, 1997; Huntley et al., 2006; Knoll et al., 2006; Xiao and Dong, 2006; Riedman et al., 2014, Cohen and Macdonald, 2015). Although these reports vary in approach, assessing binned global species richness or morphological disparity or within-assemblage diversity, they all indicate broad trends of increase in the Mesoproterozoic Era leading to a peak and then decline ~750 to 600 Ma. The resolution of these studies, however, was coarse because poor age constraints on fossiliferous units necessitated the use of broad (>100 Ma) time bins. Further, the lack of even loose age constraints for several fossiliferous units required their complete omission from such studies, inviting worry over the effects of sampling bias on resulting richness estimates.

In order to include richly fossiliferous but poorly dated units, we have utilized the biostratigraphic software package CONOP, a standard part of the Phanerozoic biostratigrapher's toolbox—notably, having been used to calibrate Ordovician and Silurian stage boundaries (Sadler et al., 2009; Cooper and Sadler, 2012; Melchin et al., 2012), sequence the end-Permian mass extinction (Shen et al. 2011), and examine at very high resolution the extinction dynamics of the Lower Paleozoic macrozooplankton (Cooper et al., 2013; Crampton et al., 2016). Because this program operates by creating a best-fit order of events, numerical age constraints, while necessary for placing this large set of ordered events within the

context of geological time, are not required of *all* fossiliferous sections. This freedom from requirements of absolute ages for all sections allowed inclusion of undated or poorly dated fossiliferous sections and thus greater potential resolution for trends in eukaryotic species richness that could eventually lead to a nuanced view of cause and consequence in biotic and abiotic events of the early to middle Neoproterozoic.

1.2 Neoproterozoic Biostratigraphy

Biostratigraphy has long been recognized as possibly useful for Neoproterozoic rocks but certainly more problematic than in the younger fossil record (Vidal, 1981a; Kaufman et al, 1992; Knoll, 1994; Butterfield and Rainbird, 1998). The more advanced state of Phanerozoic biostratigraphy has generally been achieved in familiar steps: simple lithological correlation is first replaced by recognition of a coarse succession of fossil assemblages; the assemblages are later superseded by finer zones and sub-zones, most with their bases defined by first appearance of an index taxon; and finally, in the most advanced schemes, a series of age-calibrated first-appearance datum events (FADs) is established. Progress is driven by improved resolution in the time line of known species originations (FADs) and extinctions (LADs), aided by integration of paleomagnetic reversal events and marine isotopic excursions, and corroborated by radio-isotopic dating. Numerical techniques and sequencing algorithms now enable paleobiological timelines to be built from far larger numbers of taxa and localities than the pioneers of biostratigraphy would have imagined (Sadler, 2004).

The slower progress of Neoproterozoic biostratigraphy is chiefly due to long or sparsely sampled stratigraphic ranges (Butterfield and Grotzinger, 2012). These are considerable hurdles for practical section-to-section correlation, but far less so for the construction of a global time line. Isolated faunas and stratigraphic sections that are too sparsely fossiliferous for detailed correlation with one another may, nonetheless, contribute meaningful information (e.g. proof of coexistence of taxa) to a finely resolved interregional timeline (Alroy, 1992; Sadler et al., 2014). We argue that the sum of all available Neoproterozoic information is adequate to support a global timeline of first- and last-appearances of taxa, even if information is too sparse to justify assuming that local first and last finds are the same age everywhere. For half a century (starting with Shaw, 1964) numerical and graphical methods of biostratigraphic sequencing have explicitly avoided this assumption.

Problematic taxonomy poses an additional difficulty to Neoproterozoic biostratigraphy. The dominant eukaryotic fossils of the Precambrian are acritarchs, originally sphaeroidal, organic-walled microfossils that are typically tens to hundreds of micrometers in diameter and may be smooth-walled, ornamented, or spine (process)-bearing and are of unknown biological affinity. The name 'acritarch' refers to a group of fossils united by their microscopic size and uncertain biological origins and is expected to include both vegetative and resistant resting life stages of both planktonic and benthic single-celled eukaryotes and possibly diapause cysts of animals (Knoll et al., 2006; Yin et al., 2007; Cohen et al., 2009). The question of the biological placements of these forms is not a hindrance to their use in biostratigraphy *per se*, but the lack of biological context is significant in that acritarch taxonomic hierarchy, although guided by morphology, is not necessarily

guided by synapomorphies of coherent biological groups. Because of this the treatment of acritarch richness must be made with care and typically at the species level, but with a watchful eye out for over-split genera, such as the Ediacaran *Appendisphaera*. Additionally, robust biostratigraphic correlations must be based on unique taxa or designated combinations of species rather than morphological grades (e.g., "macroalgae", "LOEM"=large ornamented Ediacaran microfossils (Cohen et al., 2009), "ELP"=Ediacaran leiosphere palynoflora and "ECAP"=Ediacaran complex acritarch palynoflora (Grey et al., 2003; see Xiao et al., 1997).

Certain Neoproterozoic species have been suggested as possible index taxa due to their wide distributions, distinctive morphological features and their ease of recognition in both thin section and acid macerate preparations. These include the acritarchs, *Cerebrosphaera globosa* (=*C. buickii*, Hill and Walter, 2000; Grey et al., 2011; see Porter and Riedman, 2016 for nomenclatural act), *Trachyhystrichosphaera aimika* (Kaufman et al., 1992; Vidal et al., 1993; Butterfield et al., 1994; Knoll, 1996; Tang et al., 2013; Xiao et al., 2016; Baludikay et al., 2016; Beghin et al., 2017) and *Lanulatisphaera laufeldii* (Porter and Riedman, 2016). These taxa are indeed globally distributed and morphologically distinctive, but as is typical of Precambrian taxa, they are also rather long-lived: *T. aimika* ranges from the late Mesoproterozoic through much of the Tonian (Tang et al., 2013; Beghin et al., 2017). *C. globosa* appears to have been somewhat shorter-lived; its oldest occurrence dates from ~800 Ma in several units of the Centralian Superbasin of Australia (Grey et al., 2011) and its youngest occurrence is between 751 and 729 Ma from the upper Chuar Group, Grand Canyon, USA (Nagy et al., 2009; Porter and Riedman, 2016; Rooney et al., *in press*). Vase-shaped microfossils (VSMs), interpreted as the remains of testate amoebae (Porter and Knoll, 2000), have also long been suggested as a possible Neoproterozoic index fauna (Knoll and Vidal, 1980; Vidal et al., 1993; Porter and Knoll, 2000; Macdonald et al., 2013, Strauss et al., 2014; Cohen et al., 2017). Individual VSM species have recently been described as composing an index assemblage typical of ~789–729 Ma due to their local abundance, global distribution in various lithofacies and short stratigraphic ranges (Riedman et al., *this issue*).

2. Methods

Here we present analyses of paleontological data from 166 formations in 60 groups of globally distributed successions (Fig. 1) as established from publications available before the end of March 2017. These data comprise reports from any fossiliferous lithofacies and include siliciclastics, carbonates and cherts (indicated in supplementary data tables). Great effort was made to include all literature addressing paleontological, radiometric, stratigraphic and geochemical data for paleogeographically units roughly 1Ga to 635 Ma in age from any language of publication. In order to allow discussion of global eukaryotic richness trends, globally distributed data are required, and on a broad scale these are seen here (Fig. 1), but the dearth of data from Africa and South America are apparent and concerning.

The analyses required stratigraphic depth information for local first and last occurrences of each taxon and careful attention to fossil identifications and

synonymies. The inclusion of radiometric ages, carbon isotopic anomalies and glacial events provided additional constraints on sequence and essential information for time calibration. Each of these data or event types is discussed in detail below and their records within each section of the database are available in Supplemental Table 1.

2.1 Paleontological data

2.1.1 Taxonomy

Although Precambrian paleontology is a rather young field, a staggering number of taxa have been named, several many times over. This is problematic for studies of species richness and is especially acute for the principal fossil group of this time, the organic-walled microfossils called acritarchs. Taphonomic and ontogenetic variations of a given species may be described under multiple names, resulting in inflation of species richness; alternatively, richness may be artificially depressed if morphological differences are lost during decay and diagenesis or are too subtle to be recognized during routine transmitted light microscopy (e.g. Porter and Riedman, 2016; Riedman and Porter, 2016; Tang et al., 2017).

During collection of species first and last occurrence data from the literature, the greatest of care was exercised in accepting, rejecting or synonymizing fossil identifications based upon species descriptions and diagnoses (see Supplementary Table 1 for list of all taxonomic decisions). Because of the importance of accurate and consistent identification for these biostratigraphic analyses, occurrences of fossil taxa were not accepted unless accompanied by convincing illustrations. Good-quality illustration was particularly important when an early find of a given species was left in open nomenclature and named in a subsequent publication. Examples of this are seen in fossils recorded as only "VSMs" or "tear-shaped fossils" that were later identified at species level (Porter et al., 2003; Riedman et al., *this issue*) and in the acritarch identified as *Kildinella* sp. by Vidal (1979; pl. 4, C and D) that was later recognized as a new genus and species (*Culcitulisphaera revelata*) with occurrences in the Chuar, Uinta Mountain and Eleonore Bay groups and Alinya Formation (Porter and Riedman, 2016; Riedman and Porter, 2016).

Fossils were included in the database only if convincingly biogenic and likely or certainly eukaryotic. With a preference toward inclusiveness, species of the smooth-walled genus *Leiosphaeridia* were included despite the concern that some of these, particularly the smaller forms i.e., *L. crassa* and *L. minutissima*, may include some prokaryotes. These species contribute nothing to ordering of events since they all range through the interval of interest (1000 to ~635 Ma), but in some units, particularly of the Cryogenian, these taxa compose the whole of the assemblage.

In addition to organic-walled acritarchs, fossil groups within this database include enigmatic scale microfossils known from the Fifteenmile Group, Yukon Territory of Canada (Allison and Hilgert, 1986; Cohen and Knoll, 2012; Cohen et al., 2017), organic macrofossil compressions such as *Longfengshania*, *Tawuia* and *Protoarenicola*, and the aforementioned vase-shaped microfossils.

2.1.2 Stratigraphic range data

Because the CONOP program utilizes local lowest and highest finds of a species, the relative stratigraphic positions of fossil occurrences were required of the primary paleontological literature. In some cases, important and diversely fossiliferous assemblages could not be included because those superpositional data were missing; for example, the well-preserved fossil assemblage of the ~1 Ga Lakhanda Group of Siberia was omitted due to a lack of stratigraphic context for the fossil occurrences. The option of treating all of a unit's reported fossil occurrences as a single sample or horizon was not acceptable because documented species co-occurrences data are a primary constraint on the permissible composite sequences. If any one unit were treated as a single sample, then all single-horizon evidence of coexistence would have to be ignored.

When possible, occurrence data from multiple studies of the same unit were combined into a single section to strengthen the local sequence (e.g., Butterfield et al. [1994] and Butterfield [2004] for the Svanbergfjellet Formation or Hofmann and Aitken [1979] and Hofmann [1985] for the Little Dal Group). Additionally, fossiliferous sections reported in separate publications but of known superpositional relationship were "stitched together". In this way the program received as much relative depth information as possible for biostratigraphic sequencing. The ability to provide such information was also useful where substantial hiatuses were known to occur within or between units. In such instances a section can be broken in two and then stitched together in a way that allows ranges that begin or end at the hiatus to be treated with the same uncertainty that attaches to range ends coincident with the top or bottom of a measured section; in other words, the span of the hiatus can be stretched to best accommodate evidence from other localities.

In the Phanerozoic studies to which CONOP has been applied, species lifetimes are typically much shorter than the depositional duration of the sections in which they are preserved. Neoproterozoic data tend to reverse this relationship; many Precambrian taxa tend to be long-lived, with ranges exceeding the time span of the fossiliferous intervals of measured sections. Our understanding of how to accommodate this condition of the Precambrian fossil record was guided by a classroom application of CONOP (Sadler, unpublished data) to a Paleozoic database of acritarchs and graptolites, an extension of work on Ediacaran and Cambrian acritarchs by Cohen (2005). This exercise illustrated that algorithm settings for long-lived acritarchs needed to be altered from those established for the shorter-lived graptolite taxa of the same age (Sadler et al., 2009). This work also indicated the importance of observed taxon coexistences in driving the solution when taxon ranges are long relative to the time spans of sections. Most Lower Paleozoic sections are sufficiently richly sampled that a strict threshold can be maintained for proof of coexistence — pairs of taxon ranges must overlap by two or more sample horizons to be treated as an observed coexistence. This strategy avoids the problem of condensed ("time-averaged") horizons. In mid-Neoproterozoic sections, however, fossiliferous horizons tend to be fewer and more widely spaced. To give the Neoproterozoic optimization sufficient leverage, we lowered the threshold of evidence for an observed coexistence to include co-occurrence at a single horizon. This allows meaningful inclusion of "sections" that are single samples (Alroy, 1992).

We reason that the time scales of likely condensation would be shorter than the time scales of both sample spacing and calibration uncertainty in the Neoproterozoic. We also increased, by a factor 10, the relative weighting of the penalty for unobserved (hypothesized) coexistences implied by a trial composite sequence.

2.2 Radiometric and Carbon Isotopic data

The ordination of fossil first and last occurrences was aided and time-calibration made possible by addition of associated radiometric ages and carbon isotopic data. These data were applied conservatively, included only if they were established from the fossiliferous sections or basinal correlations. Because the two most significant carbon isotope anomalies recorded during this interval, the Bitter Springs carbon isotopic anomaly (~811-789 Ma; Macdonald et al., 2010; Swanson-Hysell et al., 2015) and the Islay carbon isotopic anomaly (~740-732 Ma; Strauss et al., 2014; Rooney et al., 2014), are considered to be globally synchronous, the occurrences of these isotopic events in a fossiliferous unit served not only for chemostratigraphic correlation, but also acted, effectively, as an age constraint.

Both of these carbon isotopic excursions were broken into three slightly overlapping intervals for inclusion in our dataset; these include the decrease in $\delta^{13}C_{carb}$ values, the nadir or trough, and the increase to previous levels. In the decreasing and increasing intervals a portion of the base-line "typical Neoproterozoic" carbon isotopic values were included to apply conservative uncertainty ranges to different parts of the anomalies. The separate but overlapping interval approach was chosen to increase the likelihood of robust correlation (Sadler, 2012) and make it possible to utilize isotopic data even if the anomaly is truncated in a section (e.g., only the bottom and middle intervals Islay excursion are recorded in the Russøya Member of the Polarisbreen Group, Svalbard; Hoffman et al., 2012).

Geochemical and paleontological data are typically presented in separate publications; these data were integrated by utilizing stratigraphic positions of distinctive marker beds described in both paleontological and geochemical literature to determine meterage scaled to fossil occurrence depths. An example of this is seen in the extrapolated Backlundtoppen Formation and Russøya Member section derived from paleontological work by Knoll and colleagues (1989) that allowed placement of the Islay isotopic excursion from data of Hoffman et al. (2012) due to both papers' description and position of the distinctive Dartboard Dolomite Member.

2.3 Glacial Tillites

Two globally synchronous glaciations (e.g. Macdonald et al., 2010; Rooney et al., 2015) commonly referred to as the Sturtian glaciation (~716-660 Ma; Macdonald et al., 2010; Rooney et al., 2015) and Marinoan glaciation (<654-635 Ma; Hoffmann et al., 2004; Condon et al., 2005; Zhang et al. 2008; Prave et al., 2016) occurred during the early to middle Neoproterozoic Era. When glacial tillites assignable to either the Sturtian or Marinoan event occur in or are closely

associated with fossiliferous sections, they were included as additional constraints and the dates indicated above were used to time-calibrate the occurrences of events.

2.4 The CONOP Program

The CONOP program is used here to develop the best-fit hypothetical order of species first appearance and last appearance data (FAD and LAD), radiometric ages, carbon isotopic events and tillite deposits. CONOP utilizes a heuristic (trial and error) approach; because of this, each run of the program will likely find a slightly different solution, even when all starting conditions remain the same. At the start of a run of the program, events without *a priori* order (i.e. species FAD and LAD) are randomly assembled by the program with all FAD events grouped in the first half and all LAD events in the second half of the sequence. Other events are placed in known order between those ends. Because events do not occur in the same order in all local sections, CONOP seeks a composite sequence that is most parsimonious with all sections. To do this the CONOP algorithm proceeds by introducing successive changes (mutations) in a hypothetical sequence and measuring the quality of that new sequence by summing minimum local adjustments needed to make all the field data agree with that sequence. These adjustments can include extending (stretching) stratigraphic ranges of taxa or compressing (shrinking) uncertainties on placement of geochemical or glacial events (explained in more detail below). Sequence mutations must honor all known species coexistences. The quality of the mutated sequence is assessed by two criteria: 1) How much shrinking and stretching of locally observed ranges and uncertainty intervals is needed to make all sections fit the sequence; and 2) How many unobserved coexistences does it introduce? The weighted sum of these two criteria is the measure of misfit between data and the hypothetical sequence that CONOP seeks to minimize (Sadler, 2010). Mutations that reduce misfit are always kept. Most mutations that increase misfit are rejected, but in order to avoid suboptimal outcomes, some bad mutations must be accepted. The likelihood of rejecting a bad mutation increases with the size of the misfit that it adds and with the number of trials since the start of the optimization. Tolerance for bad mutations is based on an analogy with attempts to growth a flawless crystal by slow cooling; this well-established heuristic method is termed *simulated annealing* (Kirkpatrick et al., 1983).

CONOP produces multiple equally good hypothetical solutions for large and locally contradictory datasets. The differences between those solutions are caused by the underdetermined nature of the problem: there will be sets of taxon first and/or last appearances for which the local sections do not provide enough information to uniquely determine their order. This is typically due to either long-lived taxa in short sections or rare taxa that occur in too few sections. This is an unsurprisingly common occurrence in Neoproterozoic biostratigraphy given the long stratigraphic ranges of several taxa (Butterfield, 2007). Fortunately, several sections that might perform this way can be placed into stratigraphic context of "better behaved" sections. For example, the Macdonaldryggen Member of the Elbobreen Formation of Svalbard preserves only species of *Leiosphaeridia*, a tremendously long-lived form-genus, but the stratigraphic position of this unit can be linked to the more fossiliferous and informative units in the rest of the

Akademikerbreen Group + Polarisbreen Group succession, forcing the positions of the problematic section. Nevertheless, a few small irresolvable "knots" of events generate a number of equally good permutations that differ in minor details.

2.4.1 Treatment of Data Types

Within the CONOP algorithm these four types of data— biostratigraphic ranges, isotopic excursions, radiometric age constraints, and glacial sedimentary features—are assigned to three different logical categories of relative age information. The categories present different options to the algorithm that must adjust local events to fit the trial sequences. Because the local ends of species ranges are not expected to capture true origination (FAD) and extinction (LAD) events, local first and last observations of a species are biased estimators, tending to underestimate the true duration of a taxon. Accordingly, CONOP allows local biostratigraphic ranges to stretch to bring all local species successions into agreement with a single sequence of events. The composite species range includes times when the species occurs *anywhere*. The net shortfall between locally observed ranges and the hypothetical composite range is its misfit.

Glacial events and isotopic excursions, however, are better input as uncertainty intervals; the recognition of isotopic excursions, for example, depends upon the abruptness of the chemical changes and sample spacing. Glacial events are input within a local section as individual intervals, whereas an isotopic excursion is treated as three movable and overlapping intervals (e.g. fall, trough, and rise) designed to ensure a given interval will capture at least one common point in time where it occurs in all local sections. This data type is allowed to shrink to fit in a correlation, as they are purposefully input as looser depth constraints (e.g. the bottom and top intervals of a negative excursion include typical $\delta^{13}C$ values from before the fall to negative values and after the return, respectively). The composite solution estimates where that part of the glaciation or excursion is seen *everywhere*. Radiometric age data are recorded twice; the dated sample is treated as an immovable marker event in the section where it was collected and all dated events are entered as an uncertainty interval in a single age-scaled "pseudo-section" using the two-sigma analytical error. These uncertainty intervals adjust to fit by shrinking. Thus, dates may be entered whose uncertainties overlap. This allows us, for example, to include a few detrital zircon analyses that constrain maximum ages. The different freedoms to adjust these different data types are assigned in data entry so that as much information as possible is used without overstating the precision of any of it (Sadler et al., 2014).

The size of each adjustment, whether the stretch of a local taxon range or shrinkage an uncertainty interval, is measured in event levels rather than stratigraphic thickness. This strategy, now routinely adopted for Phanerozoic data, avoids the confounding influence of different accumulation rates. Other factors being equal, it gives preference to information from the most richly fossiliferous, and best sampled sections rather than the thickest sections. It enables incorporation of sections for which unit thicknesses are reported only as a range of values and reduces the precision required when aligning information from more than one publication describing the same section.

2.4.2 Buffer Regions

As an artifact of *a priori* selection of an interval of study—rather than examining the whole span of existence of the eukaryotes— taxa that originated before 1Ga have their local oldest finds artificially clustered at the beginning of our interval (or somewhat after the beginning for less than common taxa), so there is a certain amount of run-up time required to reach standing richness. This is seen in reverse at the end of an interval of interest where species LAD events cluster. Artificial truncations at arbitrary interval boundaries can create the appearance of large speciation and extinction events. To mitigate this "edge-effect" we added buffer regions by including Mesoproterozoic and Ediacaran sections to pull the spurious range-end events away from the boundaries of our interval of study (1 Ga to 635 Ma; Figs. 2–5). These buffer regions are shown in grey (Figs. 2–5) and should not be read as richness records for the Mesoproterozoic Era and Ediacaran Period due to incomplete data and the same edge-effect mentioned above.

3. Results and Discussion

3.1 Species Richness Record

Development of the species richness record proceeds from CONOP solutions in three steps, which are discussed in greater detail by Sadler and colleagues (2009). Briefly, this proceeds from the ordinal composite (discussed in section 2.4) with creation of a cumulative running total of taxon richness calculated from taxa FAD and LAD events in an ordered and equally-spaced sequence (Fig. 2A). This is the sequence that CONOP optimizes. The second step scales the spacing between events using net turnover to estimate the relative duration of sections and mean rock thickness to estimate the relative waiting time between events (Fig. 2B). This step requires simplistic assumptions about turnover and accumulation rates that are not allowed to compromise the primary sequencing; the essential aspect of this second step is that sets of events whose internal sequence is not resolvable receive zero spacing (Sadler et al., 2009). This thickness-scaled composite should look like a single hypothetical section that records all events in their order and with variable spacing that can include, for example, mass extinction horizons. Conversion from a thickness-scaled composite to an age-scaled composite sequence (Fig. 2C) relies upon dated events in the initial optimization; it proceeds by piece-wise interpolation between dated events using a cross-plot of the age-scaled pseudo-section and the thickness-scaled composite section (Fig. 3).

The species richness record presented here (Fig. 4A) overlays six best-fit calibrated richness histories utilizing the same run-time parameters and input of paleontological, carbon isotopic, radiometric and glacial data. These solutions vary because of the underdetermined nature of the problem. The heuristic approach taken by CONOP allows the set of equally well-fit solutions to be presented as an explicit and conservative band of uncertainty, together with the shape of any individual solution. The variation among solutions smears but does not wash-out essential features of the richness history. Examples can be seen with the grey and black peaks ~770 Ma (Fig. 4A) that indicate multiple FADs of taxa in the Alinya

Formation as well as grey and black peaks ~743 Ma of FADs of taxa such as *Jacutianema solubila*, *Germinosphaera* spp and *Proterocladus* spp from the upper Svanbergfjellet Fm (arrows in Figs. 4 and 5). These peaks have slightly varying placements in the six age-scaled solutions presented, but the variations are by only a few million years.

3.1.1 Major Features of species richness record

Our age-scaled species richness record shows a moderate and rather stable richness level continuing from the Mesoproterozoic into the early Neoproterozoic, as has been reported in many previous studies (e.g. Knoll, 1994; Knoll et al., 2006). A sharp richness peak is seen ~810 Ma based on new data from Cohen and colleagues (2017) that constrains the age and placement, with respect the Bitter Springs event, for the Fifteenmile scale fossils. Prior to these new data, this fossiliferous unit had been constrained to have occurred between the Bitter Springs and Islay events and the CONOP program had placed the taxa FADs and LADs nearer the Svanbergfjellet peak. Because the Fifteenmile scale taxa are still unknown from any other units their FADs and LADs provide no direction to CONOP for placement in the sequence, thus the previous, younger placement in the age-scale composite was likely due to the upsection occurrence of acritarch taxa such as *Trachyhystrichosphaera aimika* and *Cymatiosphaeroides kullingii*. This large jump of the peak indicates the power of additional age constraints and even more so, the significance of understanding the fossil unit's position relative to the Bitter Springs and Islay carbon isotopic events.

At ~800 Ma another jump in richness occurred and step-wise increase continued until a peak ~770 Ma. At this time a decline in richness began and is associated with loss of several long and short-ranging acritarch taxa (Fig. 5). This loss begins with taxa such as *Squamosphaera colonialica* (=*Satka colonialica*), *Navifusa* spp., and the problematic and possibly taphonomically derived *Tasmanites rifejicus*, and continues with loss of the shorter-ranging *Culcitulisphaera revelata* and *Vidalopalla verrucata*, and finally *Valeria lophostriata*, *Tawuia dalensis, Cerebrosphaera globosa, Lanulatisphaera laufeldii* and *Trachyhystrichosphaera aimika.* (*Simia annulare* is also lost during this interval but at the same time, the morphologically similar *Simia nerjenica* appeared. Due to unresolved taxonomic problems with the genus, the comings and goings of these taxa are given little weight.) During this broad decline in richness from ~770 to ~733 Ma there are several local peaks, the latter of which are associated with first occurrences of several vase-shaped microfossil taxa such as *Cycliocyrillium simplex* and *Melanocyrillium hexodiadema*. These vase-shaped microfossil species are short-lived, disappearing by ~733 Ma. After ~733 Ma richness values stabilized at a level lower than had been seen in the previous 500 million years; those levels remained low through the end of the Marinoan glaciation (~635 Ma).

In order to determine any influence of the uneven nature of Precambrian sample availability upon taxon richness estimates, the CONOP rarefaction algorithm (discussed in detail in Sadler, 2012) was used to produce a rarefied richness curve, standardized to a uniform sample size of 50 local ranges (with the exception of the end of the interval of study where the number of available sections was below 50 local ranges). This rarefied richness curve (Fig. 4B) echoes the major features of the

age-scaled richness curve (Fig. 4A) such as the richness increase between ~800 and 770 Ma, the broad loss of richness from ~770 to ~738, a short-lived richness increase from cameo appearances of VSM taxa, and then decline after ~733 Ma. The striking similarity of the rarefied richness curve with the non-standardized, age-scaled richness curve provides support for this solution and suggests minimal influence of uneven sampling across the interval of study. Similar trend stability was seen by Cohen and Macdonald (2015) in their investigation of the effects of lithological biases on Precambrian diversity records, providing additional support for the robustness of the Proterozoic fossil record.

These results are not completely dissimilar from those of previous studies of Precambrian species richness that reported an increase in richness between 900 and 800 Ma and a sharp drop preceding or associated with the Cryogenian glaciations (Knoll, 1994; Vidal and Moczydłowska-Vidal, 1997; Knoll et al., 2006; Cohen and Macdonald, 2015). The current study, however, benefits not only from the addition of non-paleontological data, but also from the increased resolution available by inclusion of poorly or undated fossil assemblages, data unavailable in approaches using within-assemblage richness (Knoll, 1994; Knoll et al., 2006; Cohen and Macdonald, 2015) or interval binned richness (Vidal and Moczydłowska-Vidal, 1997; Huntley et al., 2006). Here we see more detail in the initial richness increase, which is intriguingly (and at least temporally) associated with the initial stages of the Bitter Springs carbon isotopic event, and we see a more protracted loss of richness with disappearance of long-lived acritarch taxa largely preceding the appearance of vase-shaped microfossil taxa and providing support for earlier observations of apparent biotic turnover (e.g. Nagy et al., 2009). Although previously hypothesized to have been precipitated by the onset of the Sturtian glaciation, our data indicate the ~770 to ~733 Ma drop in richness—and indeed extinction, as these taxa are never again seen—occurred well before any lithological evidence of glaciation. This loss of richness, first of many acritarch taxa and later of VSMs— appears to have occurred before and then during the earliest stages of the Islay carbon isotopic excursion. In contrast to the interval of Bitter Springs anomaly, no richness increase accompanies the Islay. This would suggest that any relationship between carbon isotopic excursions and eukaryotic richness is more complex than cause and consequence. Despite occurrences of enigmatic protistan forms and macroalgae reported from interglacial and Marinoan units (Bosak et al, 2011a,b; Bosak et al., 2012; Dalton et al., 2012; Cohen et al., 2015; Ye et al 2015), a low level of species richness continued through the Sturtian and Marinoan glaciations, with richness recovering later in the Ediacaran Period with the appearance of a new suite of taxa (Knoll et al., 2006; Cohen and Macdonald, 2015).

3.2 Potential index taxa

From placements of first and last appearance events in an age-scaled, best-fit composite section, total stratigraphic ranges can be estimated for all taxa. In addition to explaining some of the features of the richness record (as discussed above), these stratigraphic range data can be considered when forming a list of potential index taxa. Because ideal index taxa should be common, globally distributed, easily and confidently identified and short-lived, few Neoproterozoic

taxa fit the bill. Stratigraphic ranges for morphologically distinct taxa that appear in four or more sections within the database with no significant gaps or outliers are illustrated in Figure 5.

Although none of the potential Neoproterozoic index taxa previously suggested in the literature or discovered during this study can approach the Phanerozoic standard for index fossils in terms of numbers of reported occurrences or time-restricted stratigraphic range, several species do appear to have strong potential biostratigraphic utility. These include *Cerebrosphaera globosa* (=*C. buickii*; Hill et al., 2000; Grey et al., 2011), vase-shaped microfossil taxa such as *Cycliocyrillium simplex* or *Melanocyrillium hexodiadema* (VSMs; Porter and Knoll, 2000; Strauss et al., 2014; Riedman et al., *this issue*) and to a lesser extent, *Trachyhystrichosphaera aimika* (Vidal et al., 1993; Butterfield et al., 1994; Samuelsson and Butterfield, 2001; Srivastava, 2009; Tang et al., 2013).

Cerebrosphaera globosa is a cosmopolitan, distinctively wrinkled and robust-walled acritarch that is easily recognizable in both acid macerations of siliciclastics and in thin sections of chert (Porter and Riedman, 2016); it is also one of the most commonly suggested index fossil candidates (e.g. Hill and Walter, 2000; Grey et al., 2011). The oldest finds of *C. globosa* are estimated to be ~800 Ma from the Centralian Basin of Australia (Grey et al., 2011) and the youngest are from the Chuar Group, USA and dated to be between 751 and 729 Ma (Nagy et al., 2009; Porter and Riedman, 2016; Rooney et al., *in press*). This taxon's stratigraphic range as derived from the CONOP age-scaled composite (Fig. 5) is estimated to be somewhat tighter, from ~792 to 738 Ma, providing even greater support for this taxon as an important biostratigraphic element.

Trachyhystrichosphaera aimika has also received a great deal of attention as a possible index taxon (Kaufman et al., 1992; Vidal et al., 1993; Butterfield et al., 1994; Knoll, 1996; Tang et al., 2013; Xiao et al., 2016; Baludikay et al., 2016; Beghin et al., 2017); it is a large (up to 700 μm in diameter), process-bearing acritarch found in both siliciclastics and cherts world-wide. Paleontological reports and radiometric data constrain this taxon to between ~1.1 Ga and ~750 Ma based on occurrences in the Atar El Mreïti Group, Democratic Republic of Congo (Beghin et al., 2017; Rooney et al., 2010) and the Kwagunt Formation of the Chuar Group (Porter and Riedman, 2016) and Draken Formation (=*T. vidalii*; Knoll et al., 1991). The stratigraphic range estimate of *T. aimika* is from ~1.1 Ga (based on radiometric constraints on occurrences) to between 743 and 738 Ma (Fig. 5) according to CONOP's age-scaled composite. The uncertainty in this LAD (expressed as a dotted line in Fig. 5) is due to the occurrence of an outlier at ~738 Ma, namely, the occurrence of *T. aimika* in the stratigraphically well-constrained but undated Draken Formation, Svalbard (Knoll et al., 1991). This is the only instance of this taxon, or indeed any of the complex Tonian acritarch taxa, co-occurring with vase-shaped microfossil taxa. The stratigraphic range estimate of *T. aimika* suggests that on its own, this taxon is too long-ranging for its fossil find to be of significant biostratigraphic use in constraining host rock age.

Vase-shaped microfossils have also been put forth as possible index taxa for a number of years (Knoll and Vidal, 1980; Porter and Knoll, 2000; Porter et al., 2003; Strauss et al., 2014; Cohen et al., 2017; Riedman et al., *this issue*). These are

morphologically distinct taxa that appear in various lithofacies in a variety of preservational modes and they have a broad paleogeographic distribution. The stratigraphic ranges of VSM taxa such as *Cycliocyrillium simplex* are constrained by paleontological, radiometric and carbon isotopic events to be ~789 Ma to ~729 Ma based on FADs that all post-date the end of the Bitter Springs carbon isotopic anomaly and the youngest occurrence below the dated tuff of the upper Chuar Group ~729 Ma (Porter et al., 2003; Rooney et al., *in press*; Riedman et al., *this issue*). The CONOP age-scaled composite suggests the possibility of an even shorter range of ~760 to ~733 Ma (Fig. 5), providing additional support for use of an individual VSM taxon or an assemblage of VSM taxa as biostratigraphic markers of the late Tonian.

Finally, other morphologically distinctive acritarch species such as *Lanulatisphaera laufeldii*, *Cymatiosphaeroides kullingii*, *Culcitulisphaera revelata* and *Vidalopalla verrucata* may also be found to have strong biostratigraphic potential but at this point—the last two species especially—have too few occurrences for broad application or for strong confidence in their stratigraphic ranges. A likely eventual Neoproterozoic biostratigraphic solution is construction of one or more assemblage zones including the taxa mentioned above and taking advantage of commonly co-occurring taxa and the relative positions of their FADs and LADs.

Returning to our earlier characterization of the progress of Phanerozoic biostratigraphy, we have shown that the Neoproterozoic fossil record is sufficient to support a global paleobiological timeline that integrates information in the manner of the most advanced stage of Phanerozoic biostratigraphy. The biotic turnover is neither sufficiently rapid, nor sufficiently thoroughly preserved, however, that we can advocate treating local first appearances as correlative FADs. Rather, section-to-section and section-to-composite correlation remains at the level of coarse assemblages.

4. Conclusions

Paleontological, geochemical, sedimentological and radiometric data from 166 globally distributed formations have been combined and analyzed using the CONOP seriation algorithm, resulting in a high-resolution eukaryotic species richness record for the early to middle Neoproterozoic Era (1 Ga to 635 Ma). Major features of this record include an increase in species richness ~800 Ma, which continued to a richness peak ~770 Ma, followed by a decline from ~770 to ~733 Ma, which was fueled by losses of long and short-ranging complex acritarch taxa. During this broad decline in richness the iconic Neoproterozoic vase-shaped microfossil taxa appear and disappear. By ~733 Ma richness values fell to—and maintained for an extended time—levels lower than recorded for the previous half-billion years, not returning to previous levels until the rise of Ediacaran acritarch taxa after the end of the second Cryogenian glacial event.

These analyses permit estimation of stratigraphic ranges of all taxa, useful not only for providing insight into the features of the richness record, but also for objectively seeking biostratigraphic index taxa for this interval. From these analyses several species appear to be of potential importance in Neoproterozoic

biostratigraphy—in particular, *Cerebrosphaera globosa* and vase-shaped microfossil taxa such as *Cycliocyrillium simplex* species are especially well supported.

Acknowledgements

The authors thank Phoebe Cohen, Timothy Gibson, Sarah Wörndle-Quoëx and Alan Rooney for the much appreciated access to their prepublication data. The authors also thank Susannah Porter, Andrew Knoll, Bruce Tiffney and Stan Awramik for constructive comments on earlier drafts of the manuscript, and we thank Phoebe Cohen and Shuhai Xiao for their insightful and helpful reviews. This work would have been impossible without help from an army of librarians, interlibrary loan and the Biodiversity Heritage Library. This work was supported by a NASA Astrobiology Postdoctoral Fellowship (to L.A.R.). Development of CONOP was funded, in part, by NSF grants EAR 9980371, EAR 0518939, and OPP 0338274 (to P.S.).

References Cited

Allison, C. W. and Awramik, S., 1989, Organic-walled microfossils from the earliest Cambrian or latest Proterozoic Tindir Group rocks, northwestern Canada: Precambrian Research, v. 43, p. 253–294.

Allison, C. W. and Hilgert, J. W., 1986, Scale microfossils from the early Cambrian of Northwest Canada: Journal of Paleontology, v. 60, p. 973–1015.

Alroy, J., 1992, Conjunction among taxonomic distributions and the Miocene mammalian biochronology of the Great Plains, Paleobiology, v. 18, p. 326-343.

Amard, B., 1984, Nouveaux elements de datation de la couverture protérozoïque du craton ouest-africain: un assemblage de microfossiles (Acritarches) caractéristique du Riphéen supérieur dans la formation d'Atar (Mauritainie): Comptes Rendus de l'Académie des Sciences, Paris Série II, v. 299, p. 1405–1410. (In French)

Amard B. and Affaton, P. 1984, Découverte de *Chuaria circularis* (Acritarche) dans le basin des Volta (Haute Volta et Bénin, Afrique de l'Ouest), Age protérozoïque terminal de la formation de la Pendjari et de la tillite sous-jacente: Comptes Rendus de l'Académie des Sciences, Paris Série II, v. 299, p. 975–980. (In French)

Ambrose, G. J., Dunster, J. D., Munson, T. J. and Edgoose, C. J., 2010, Well completion report for NTGS stratigraphic drillholes LA05DD01 and BR05DD01, southwestern Amadeus Basin: NT Geological Survey, Record 2010-015.

Baludikay, B. K., Storme, J. -Y., François, C., Baudet, D., Javaux, E. J., 2016, A diverse and exquisitely preserved organic-walled microfossil assemblage form the Meso-Neoproterozoic Mbuji-Mayi Supergroup (Democratic Republic of Congo) and implications for Proterozoic biostratigraphy, Precambrian Research, v.281, p. 166–184.

Beghin, J., Storme, J-Y., Blanpied, C., Gueneli, N., Brocks, J., Poulton, S. W., Javaux, E. J., 2017, Microfossils from the late Mesoproterozoic-early Neoproterozoic Atar/ El Mreïti Group, Taoudeni Basin, Mauritania, northwestern Africa: Precambrian Research, v. 291, p 63–82.

Bold, U., Crowley, J. L., Smith, E. F., Sambuu, O., Macdonald, F. A., 2016, Neoproterozoic to early Paleozoic tectonic evolution of the Zavkhan terrane of Mongolia: implications for continental growth in the Central Asian orogenic belt: Lithosphere, v. 8, p. 729–750.

Bosak, T., Macdonald, F., Lahr, D., Matys, E., 2011a, Putative Cryogenian ciliates from Mongolia: Geology, v., 39, p. 1123–1126.

Bosak, T., Lahr, D. J. G., Pruss, S. B., Macdonald, F. A., Dalton, L., Matys, E., 2011b, Agglutinated tests in post-Sturtian cap carbonates of Namibia and Mongolia: Earth and Planetary Science Letters, v. 308, p. 29–40.

Bosak, T., Lahr, D., J., G., Pruss, S. P., Macdonald, F. A., Gooday, A. J., Dalton, L., Matys, E., 2012, Possible early foraminiferans in post-Sturtian (716-635 Ma) cap carbonates: Geology, v. 40, p. 67–70.

Butterfield, N. J., 2004, A vaucheriacean alga from the middle Neoproterozoic of Spitsbergen: implications for the evolution of Proterozoic eukaryotes and the Cambrian explosion: Paleobiology, v. 30, p. 231–252.

Butterfield, N. J., 2005a, Reconstructing a complex early Neoproterozoic eukaryote, Wynniatt Formation, arctic Canada: Lethaia, v. 38, p. 155–169.

Butterfield, N. J., 2005b, Probably Proterozoic Fungi: Paleobiology, v. 31, p. 165–182.

Butterfield, N. J., 2007, Macroevolution and macroecology through deep time: Palaeontology, v. 50, p. 41–55.

Butterfield, N. J. and Grotzinger, J. P., 2012, Palynology of the Huqf Supergroup, Oman, *in* Bhat, G. M., Craig, J. Thurow, J. W., Thusu, B. and Cozzi, A. (eds.) Geology and Hydrocarbon Potential of Neoproterozoic–Cambrian Basins in Asia Geological Society of London Special Publications, v. 366, p. 251–263.

Butterfield, N. J., Knoll, A. H. and Swett, K., 1994, Paleobiology of the Neoproterozoic Svanbergfjellet Formation, Spitsbergen: Fossils and Strata, no. 34, p. 1–84.

Butterfield, N. J. and Rainbird, R. H., 1998, Diverse organic-walled fossils, including "possible dinoflagellates", from the early Neoproterozoic of arctic Canada: Geology, v. 26, p. 963–966.

Cahen, L., Snelling, N. J, Delhal, J., Vail, J. R., 1984, The geochronology and evolution of Africa, Clarendon Press, 512pp.

Calver, C., 2011, Neoproterozoic glacial deposits of Tasmania, *in* Arnaud, E., Halverson, G. P., Shields-Zhou, G., (eds.), The Geological Record of Neoproterozoic Glaciations: Geological Society of London Memoirs, no. 36, p. 649–657.

Canfield, D. E., 2014, Oxygen: a four billion year history: Princeton University Press, 224 p.

Cohen, P. A., 2005, High Resolution biostratigraphic correlation of acritarch diversity in the Neoproterozoic and earliest Cambrian using CONOP9, Geological Society of America Abstracts with Programs, v. 37(7), p. 369

Cohen, P. A. and Knoll, A. H., 2012, Scale microfossils from the mid-Neoproterozoic Fifteenmile Group, Yukon Territory: Journal of Paleontology, v. 86, p. 775–800.

Cohen, P. A., Knoll. A. H., Kodner, R. B., 2009, Large spinose microfossils in Ediacaran rocks as resting stages of early animals: Proceedings of the National Academy of Sciences, v. 106, p. 6519–6524.

Cohen, P. A. and Macdonald, F. A., 2015, The Proterozoic record of eukaryotes: Paleobiology, v. 41, p. 610–632.

Cohen, P. A., Macdonald, F. A., Pruss, S. B., Matys, E., Bosak, T., 2015, Fossils of putative marine algae form the Cryogenian glacial interlude of Mongolia: Palaios, v. 30, p., 238–247.

Cohen, P. A., Tosca, N., Rooney, A., Sharma, M., Strauss, J. V., 2017 Controlled hydroxyapatite biomineralization in an ~810 million year olds unicellular eukaryote: Science Advances 3, e1700095.

Condon, D. J., Zhu, M., Bowring, S., Wang, W., Yang, A. and Jin, Y., 2005, U-Pb ages from the Neoproterozoic Doushantuo Formation, China: Science, v. 308, p. 95–98.

Cooper, R.A., and Sadler, P.M., 2012, The Ordovician Period, in Gradstein, F., Ogg, J, G., Schmitz, M., and Ogg, G., (eds.) Geologic Time Scale 2012, volume 2, p. 500-534, Elsevier.

Cooper, R.A., Sadler, P.M., and Munnecke, A., Crampton, J.S., 2013, Graptoloid evolutionary rates track Ordovician-Silurian climate change: Geological Magazine, v. 151(2), p.349-364.

Cotter, K., 1997, Neoproterozoic microfossils from the Officer Basin, Western Australia: Alcheringa, v. 21, p. 247–270.

Cotter, K., 1999, Microfossils from Neoproterozoic Supersequence 1 of the Officer Basin, Western Australia: Alcheringa, v. 23, p. 63–86.

Couëffé, R. and Vecoli, M., 2011, New sedimentological and biostratigraphic data in the Kwahu Group (Meso- to Neo-Proterozoic), southern margin of the Volta Basin, Ghana: stratigraphic constraints and implications on regional lithostratigraphic correlations: Precambrian Research, v. 189, p. 155–175.

Crampton, J.S., Cooper, R.A., Sadler, P.M., and Foote, M., 2016, Greenhouse-icehouse transition in the Late Ordovician marks a step change in extinction regime in the marine plankton: Proceedings of the National Academy of Science, v. 113, p.1498-1503.

Dalton, L. A., Bosak, T., Macdonald, F. A., Lahr, D. J. G., Pruss, S. B., 2012, Preservational and morphological variability of assemblages of agglutinated eukaryotes in Cryogenian cap carbonates of northern Namibia; Palaios, V. 28, p. 67–79.

Dehler, C.M., Gehrels, G., Porter, S.M., Cox, G., Heizler, M.T., Karlstrom, K.E., and Crossey, L.J., 2014, ChUMP (Chuar-Uinta Mountain-Pahrump) strata of the western U.S. record Cretaceous-like ocean anoxia events (OAEs) before Snowball Earth: Geological Society of America Abstracts with Programs, v. 46, p. 627.

Dehler, C. M., Porter, S. M., De Grey, L. D., Sprinkel, D. A. and Brehm, A., 2007, The Neoproterozoic Uinta Mountain Group revisited: a synthesis of recent work on the Red Pine Shale and related undivided clastic strata, northeastern Utah, USA *in* Proterozoic Geology of Western North America and Siberia: SEPM Special Publication 86, p. 151–166.

Dong, L., Xiao, S., Shen, B., Yuan, X., Yan, X. and Peng, Y., 2008, Restudy of the worm-like carbonaceous compression fossils *Protoarenicola*, *Pararenicola*, and *Sinosabellidites* from early Neoproterozoic successions in North China: Palaeogeography, Palaeoclimatology, Palaeoecology, v. 258, p. 138–161.

Du, Rulin and Tian Lifu, 1985, Algal macrofossils from the Qingbaikou System in the Yanshan Range of North China: Precambrian Research, v. 29, p. 5–14.

François, C., Baludikay, B. K., Storme, J.-Y, Baudet, D., Javaux, E. J., 2015 Geochronological constraints on the diagenesis of the Mbuji-Mayi Supergroup, Democratic Republic of Congo (DRC). In: Goldschmidt Annual Meeting, Prague, August 16-21, Abstract #937.

Gibson, T., in prep. (New age constraints on Angmaat Formation, Bylot Group)

Grey, K., 1999, Proterozoic palynology of samples from Empress 1A, *in* Stevens, M. K. and Apak, S. N., (eds.), GSWA Empress1 and 1A well completion report Yowalga Sub-

basin, Officer Basin, Western Australia: Geological Survey of Western Australia, record 1999/4, p. 68–69.

Grey, K., Hill, A. C. and Calver, C., 2011, Biostratigraphy and stratigraphic subdivision of Cryogenian successions of Australia in a global context, *in* Arnaud, E., Halverson, G. P. and Shields-Zhou, G. (eds.) The Geological Record of Neoproterozoic Glaciations: Geological Society, London, Memoirs, no. 36, p. 113–134.

Grey, K., Walter, M. and Calver, C. 2003, Neoproterozoic biotic diversification: Snowball Earth or aftermath of the Acraman impact?: Geology, v. 31, p. 459–462.

Halverson, G. P., Hoffman, P. F., Schrag, D. P., Maloof, A. C. and Rice, A. H. N., 2007, Toward a Neoproterozoic composite carbon-isotope record: GSA Bulletin, v. 117, p. 1181–1207.

Heaman, L. M., LeCheminant, A. N., Rainbird, R. H., 1992, Nature and timing of Franklin igenous events, Canada: Implications for a late Proterozoic mantle plume and the break-up of Laurentia: Earth and Planetary Sciences Letters, v. 109, 117-131.

Hill, A. C., Cotter, K. L. and Grey, K., 2000, Mid-Neoproterozoic biostratigraphy and isotope stratigraphy in Australia: Precambrian Research, v. 100, p. 281–298.

Hill, A. C. and Walter, M. R., 2000, Mid-Proterozoic (~830–750 Ma) isotope stratigraphy of Australia and global correlation: Precambrian Research, v. 100, p. 181–211.

Hoffman, P. F., Halverson, G. P., Domack, E. W., Maloof, A. C., Swanson-Hysell, N. L. and Cox, G., 2012, Cryogenian glaciations on the southern tropical paleomargin of Laurentia (NE Svalbard and East Greenland), and a primary origin for the upper Russøya (Islay) carbon isotope excursion: Precambrian Research, v. 206–207, p. 137–158.

Hoffman, P. F. and Li, Z-X., 2009, A palaeogeographic context for Neoproterozoic glaciation: Palaeogeography, Palaeoclimatology, Palaeoecology, v. 277, p158–172.

Hofmann, H. J., 1985, The mid-Proterozoic Little Dal Macrobiota, Mackenzie Mountains, north-west Canada: Palaeontology, v. 28, p. 331–354.

Hofmann, H. J., 1999, Global distribution of the Proterozoic sphaeromorph acritarch *Valeria lophostriata* (Jankauskas): Acta Micropalaeontologica Sinica, v. 16, p. 215–224.

Hofmann, H.J. and Aitken, J. D., 1979, Precambrian biota from the Little Dal Group, Mackenzie Mountains, northwestern Canada: Canadian Journal of Earth Sciences, v. 16, p. 150–166.

Hofmann, H. J. and Jackson, G. D., 1994, Shale-facies microfossils from the Proterozoic Bylot Supergroup, Baffin Island, Canada: Paleontological Society Memoir, no. 37, p. 1–39.

Hofmann, H. J. and Rainbird, R. H., 1995, Carbonaceous megafossils from the Neoproterozoic Shaler Supergroup of Arctic Canada: Palaeontology, v. 37, p. 721–731.

Hong, T-Q, Jia, Z-H, Yin, L-M and Zheng, W-W, 2004, Acritarchs from the Neoproterozoic Jiuliqiao Formation, Huainan region, and their biostratigraphic significance: Acta Palaeontologica Sinica, v. 43, p. 377–387.

Huntley, J. W., Xiao, S. and Kowalewski, M., 2006, 1.3 Billion years of acritarch history: An empirical morphospace approach: Precambrian Research, v. 144, p. 52–68.

Jankauskas, T. V., 1978, Riphean plant microfossils from the southern Urals: Doklady Akademii Nauk SSSR, v. 242, p. 98–100 (in Russian).

Jankauskas, T. V., 1979, Middle Riphean microbiota of the southern Urals and the Ural region of Bashkiria: Doklady Akademii Nauk SSSR, v. 248, p. 190–193 (in Russian).

Jankauskas, T. V., 1982, Microfossils of the Riphean of the South Urals, *in* Keller, B. M. (ed.) Stratotype of Riphean paleontology, paleomagnetism, p. 84–120, 20 plates (in Russian)

Jankauskas, T. V., Mikhailova, N. S. and Hermann, T. N. (eds.), 1989. Mikrofossilii Dokembria SSSR: Nauka, Leningrad, p. 191. (In Russian)

Jones, D. S., Maloof, A. C., Hurtgen, M. T., Rainbird, R. H., Schrag, D. P., 2010, Regional and global chemostratigraphic correlation of the early Neoproterozoic Shaler Supergroup, Victoria Island, Northwestern Canada: Precambrian Research, v. 181, p. 43-63.

Karlstrom. K, Bowring, S., Dehler, C., Knoll, A. H., Porter, S., Des Marais, D., Weil, A., and Sharp, Z., 2000, Chuar Group of the Grand Canyon: record of breakup of Rodinia, associated change in the global carbon cycle, and ecosystem expansion by 740 Ma: Geology, v. 28, p. 619–622.

Kaufman, A. J., Knoll, A. H. and Awramik, S. M., 1992, Biostratigraphic and chemostratigraphic correlation of Neoproterozoic sedimentary succession: Upper Tindir Group, northwestern Canada, as a test case: Geology, v. 20, p. 181–185.

Kendall, B., Creaser, R., Calver, C. R., Raub, T. D. and Evans, D. A. D., 2009, Correlation of Sturtian diamictite successions in southern Australia and northwestern Tasmania by Re-Os black shale geochronology and the ambiguity of "Sturtian"-type diamictite-cap carbonate pairs as chronostratigraphic marker horizons: Precambrian Research, v. 172, p. 301–310.

Kendall, B., Creaser, R. A. and Selby, D., 2006, Re-Os geochronology of postglacial black shales in Australia: constraints on the timing of "Sturtian" glaciation: Geology, v. 34, p. 729–732.

Kirkpatrick, S., Gelatt, C. D., and Vecchi, M. P., 1983, Optimization by Simulated Annealing: Science, v.220(4598), p. 671–680. doi:10.1126/science.220.4598.671

Knoll, A. H., 1984, Microbiotas of the Late Precambrian Hunnberg Formation, Nordaustlandet, Svalbard: Journal of Paleontology, v. 58, p. 131–162.

Knoll, A., 1994, Proterozoic and early Cambrian protists: evidence for accelerating evolutionary tempo: Proceedings of the National Academy of Sciences, v. 91, p. 6743–6750.

Knoll, A. H., 1996, Chapter 4: Archean and Proterozoic paleontology, p. 51–80. *In* J. Jansonius and D. C. McGregor (eds.), Palynology: principles and applications. American Association of Stratigraphic Palynologists Foundation, Vol 1.

Knoll, A. H. and Calder, S., 1983, Microbiotas of the Late Precambrian Ryssö Formation, Nordaustlandet, Svalbard: Palaeontology, v. 26, p. 467–496.

Knoll A. H., Javaux, E. J., Hewitt, D. and Cohen, P., 2006, Eukaryotic organisms in Proterozoic oceans: Philosophical Transactions of the Royal Society B, v. 361, p. 1023–1038.

Knoll A. H., Lahr, D. J. G., 2016, Fossils, Feeding and the evolution of complex multicellularity *in* Multicellularity: Origins and Evolution, Niklas, K. J., Newman, S. A. (eds.) MIT Press. p. 3–16

Knoll, A. H. and Swett, K., 1985, Micropaleontology of the late Proterozoic Veteranen Group, Spitsbergen: Palaeontology, v. 28, p. 51–53.

Knoll, A. H., Swett, K. and Burkhardt, E., 1989, Paleoenvironmental distribution of microfossils and stromatolites in the upper Proterozoic Backlundtoppen Formation, Spitsbergen: Journal of Paleontology, v. 63, p. 129–145.

Knoll, A. H., Swett, K. and Mark, J., 1991, Paleobiology of a Neoproterozoic tidal flat/lagoonal complex: The Draken Conglomerate Formation, Spitsbergen: Journal of Paleontology, v. 65, p. 531–570.

Knoll, A. H. and Vidal, G., 1980, Late Proterozoic vase-shaped microfossils from the Visingsö Beds, Sweden: Geologiska Föreningens I Stockholm Förhanlingar, v. 102, p. 207–211.

Li, Z. X., Bogdanova, S. V., Collins, A. S., Davidson, A., De Waele, B., Ernst, R. E., Fitzsimons, I. C. W., Fuck, R. A., Gladkochub, D. P., Jacobs, J., Karlstrom, K. E., Lu, S.. Natapov, L. M., Pease, V., Pisarevsky, S. A., Thrane, K. and Vernikovsky, V., 2008, Assembly, configuration, and break-up history of Rodinia: a synthesis: Precambrian Research, v. 160, p. 179–210.

Li, Z-X., Evans, D. A. D. and Halverson, G. P., 2013, Neoproterozoic glaciations in a revised global palaeogeography from the breakup of Rodinia to the assembly of Gondwanaland: Sedimentary Geology, v. 294, p. 219–232.

Macdonald, F. A., Jones, D. S., Schrag, D., 2009 Stratigraphic and tectonic implications of a newly discovered glacial diamictite cap carbonate couplet in southwestern Mongolia, v. 37, p. 123–126.

Macdonald, F. A., Prave, A. R., Petterson, R., Smith, E. F., Pruss, S., Oates, K., Waechter, F., Trotzuk, D. and Fallick, A. E., 2013, The Laurentian record of Neoproterozoic glaciation, tectonism, and eukaryotic evolution in Death Valley, California: GSA Bulletin, v. 125, p. 1203–1223.

Macdonald, F. A., Schmitz, M. D., Crowley, J. L., Roots, C. F., Jones, D. S., Maloof, A. C., Strauss, J. V., Cohen, P. A., Johnston, D. T. and Schrag, D. P., 2010, Calibrating the Cryogenian: Science, v. 327, p. 1241–1243.

Macdonald, F. A., Smith, E. F., Strauss, J. V., Cox, G. M., Halverson, G. P. and Roots, C. F., 2011, Neoproterozoic and early Paleozoic correlations in the western Ogilvie Mountains, Yukon, *in* MacFarlane, K. E., Weston, L. H. and Relf, C. (eds.) Yukon Exploration and Geology 2010: Yukon Geological Survey, p. 161–182.

Martí Mus, M. and Moczydłowska, M., 2000, Internal morphology and taphonomic history of the Neoproterozoic vase-shaped microfossils from the Visingsö Group, Sweden: Norsk Geologisk Tidsskrift, v. 80, p. 213–228.

McFadden, K., Xiao, S., Zhou, C. and Kowalewski, M., 2009, Quantitative evaluation of the biostratigraphic distribution of acanthomorphic acritarchs in the Ediacaran Doushantuo Formation in the Yangtze Gorges area, South China: Precambrian Research, v. 173, p. 170–190.

McKenzie, N.R., Hughes, N.C., Myrow, P.M., Xiao, S. and Sharma, M., 2011, Correlation of Precambrian-Cambrian sedimentary successions across northern India and the utility of isotopic signatures of Himalayan lithotectonic zones, Earth and Planetary Science Letters, v.312, p. 471-483.

Melchin, M.J., Sadler, P.M., and Cramer, B.D., 2012, The Silurian Period, *in* Gradstein, F., Ogg, J, G., Schmitz, M., and Ogg, G., (eds) Geologic Time Scale 2012, v. 2, p 536-569, Elsevier.

Meyer, K. M. and Kump, L. R., 2008, Oceanic euxinia in Earth history: causes and consequences: Annual Review of Earth and Planetary Sciences, v. 36, p. 251–288.

Moczydłowska, M., Pease, V., Willman, S., Wickström, L., and Agić, H., 2017, A Tonian age for the Visingsö Group in Sweden constrained by detrital zircon dating and biochronology: implications for evolutionary events: Geological Magazine, DOI: https://doi.org/10.1017/S0016756817000085

Nagy R. M. and Porter, S. M., 2005, Paleontology of the Neoproterozoic Uinta Mountain Group, *in* Dehler, C. M., Pederson, J. L., Sprinkel, D. A. and Kowallis, B. J. (eds.), Uinta Mountain geology: Utah Geological Association Publication, v. 33, p. 49–62.

Nagy, R. M., Porter, S. M., Dehler, C. M. and Shen, Y., 2009, Biotic turnover driven by eutrophication before the Sturtian low-latitude glaciation: Nature Geoscience, v. 2, 415–418.

Nyberg, A. V. and Schopf, J. W., 1984, Microfossils in stromatolitic cherts from the upper Proterozoic Min'yar Formations, southern Ural Mountains, USSR: Journal of Paleontology, v. 58, p. 738–772.

Parfrey, L. W., Lahr, D. J. G., Knoll, A. H. and Katz, L. A., 2011, Estimating the timing of early eukaryotic diversification with multigene molecular clocks: Proceedings of the National Academy of Sciences, v. 108, p. 13624–13629.

Petrov, P. Yu and Veis, A. F., 1995, Facial-ecological structure of the Derevnya Formation microbiota: upper Riphean, Turukhansk Uplift, Siberia: Stratigraphy and Geological Correlations, v. 3, p. 435–460.

Porter, S. M., 2011, The rise of predators: Geology, v. 39, p. 607–608.

Porter, S. M., 2016, Tiny vampires in ancient seas: evidence for predation via perforation in fossils from the 780–740 million-year-old Chuar Group, Grand Canyon, USA: Proceedings of the Royal Society B, v. 283: 20160221

Porter, S. M. and Knoll, A. H., 2000, Testate amoebae in the Neoproterozoic Era: evidence form vase-shaped microfossils in the Chuar Group, Grand Canyon: Paleobiology, v. 26, p. 360–385.

Porter, S. M., Meisterfeld, R. and Knoll, A. H., 2003, Vase-shaped microfossils from the Neoproterozoic Chuar Group, Grand Canyon: a classification guided by modern testate amoebae: Journal of Paleontology, v. 77, p. 409–429.

Porter S. M. and Riedman, L. A., 2016, Systematics of organic-walled microfossils from the mid-Neoproterozoic Chuar Group, Grand Canyon, Arizona: Journal of Paleontology, v. 90, p. 815–853.

Prasad. B., Uniyal, S. N. and Asher, R., 2005, Organic-walled microfossils from the Proterozoic Vindhyan Supergroup of Son Valley, Madhya Pradesh, India: Palaeobotanist, v. 54, p. 13–60.

Prave, A. R., Condon, D. J., Hoffmann, K. H., Tapster, S. and Fallick, A. E., 2016, Duration and nature of the end-Cryogenian (Marinoan) glaciation: Geology, v. 44, p. 631–634.

Qian, M-P, Jiang, Y. and Yu, M-G., 2009, Neoproterozoic millimetric-centimetric carbonaceous fossils form northern Anhui and Jiangsu, China: Acta Palaeontologica Sinica, v. 48, p. 74–88.

Riedman, L. A., Porter, S. M., Halverson, G. P., Hurtgen, M. T. and Junium, C. 2014, Organic-walled microfossil assemblages from glacial and interglacial Neoproterozoic units of Australia and Svalbard: Geology, v. 42, p. 1011–1014.

Riedman, L.A. and Porter, S.M., 2016, Organic-walled microfossils of the mid-Neoproterozoic Alinya Formation, Officer Basin, Australia: Journal of Paleontology, v. 90, p. 854–887.

Riedman, L. A., Porter, S. M. Calver, C. R., *this issue*, Vase-shaped microfossil biostratigraphy with new data from Tasmania, Svalbard, Greenland, Sweden and the Yukon: Precambrian Research.

Rooney, A. D., Austermann, J., Smith, E. F., Yang, L. Selby, D., Dehler, C. M., Schmitz, M. D., Karlstrom, K. E. and Macdonald, F. A., in press, Coupled Re-Os and U-Pb geochronology of the Tonian Chuar Group, Grand Canyon. Geological Society of America Bulletin.

Rooney A. D., Macdonald, F. A., Strauss, J. V., Dudás, F. Ö., Hallmann, C. and Selby, D., 2014, Re-Os geochronology and coupled Os-Sr isotope constraints on the Sturtian snowball Earth: Proceedings of the National Academy of Sciences, v. 111, p. 51–56.

Rooney, A. D., Selby, D., Houzay, J-P. and Renne, P. R., 2010, Re-Os geochronology of a Mesoproterozoic sedimentary succession, Taoudeni Basin, Mauritania: implications for basin-wide correlations and Re-Os organic-rich sediments systematics: Earth and Planetary Science Letters, v. 289, p. 486-496.

Rooney, A. D., Strauss, J. V., Brandon, A. D. and Macdonald, F. A., 2015, A Cryogenian chronology: two long-lasting synchronous Neoproterozoic glaciations: Geology, v. 43, p. 459–462.

Sadler, P. M., 2004, Quantitative biostratigraphy – achieving finer resolution in global correlation, Annual Reviews of Earth and Planetary Science, v. 32, p. 187-213.

Sadler, P. M., 2010a, Brute-force biochronology: sequencing paleobiologic first- and last-appearance events by trial-and-error, *in* Alroy, J. and Hunt, G. (eds.), Quantitaive Methods in Paleobiology: Paleontological Society short course, Paleontological Society Papers, v. 16, p. 271–289.

Sadler, P. M., 2010b, Biochronology as a traveling salesman problem: introduction to the CONOP9 Seriation programs. University of California, Riverside. Published online at http://www.paleosoc.org/shortcourse2010/extended-CONOP-COURSE-NOTES.pdf. 79pp

Sadler, P. M., 2012, Integrating carbon isotopic excursions into automated stratigraphic correlation: an example from the Silurian of Baltica: Bulletin of Geosciences, v. 87, p 681–694.

Sadler, P. M., Cooper, R. A. and Crampton, J. S., 2014, High-resolution geobiologica time-lines: progress and potential, fifty years after the advent of graphic correlation: The Sedimentary Record, v. 12, p. 4–9.

Sadler, P. M., Cooper, R. A. and Melchin, M., 2009, High-resolution, early Paleozoic (Ordovician-Silurian) time scales: GSA Bulletin, v. 121, p. 887–906.

Samuelsson, J., 1997, Biostratigraphy and palaeobiology of early Neoproterozoic strata of the Kola peninsula, Northwest Russia: Norsk Geologisk Tidsskrift, v. 77, p. 165–192.

Samuelsson, J. and Butterfield, N. J., 2001, Neoproterozoic fossils from the Franklin Mountains, northwestern Canada: stratigraphic and palaeobiological implications: Precambrian Research, v. 107, p. 235–251.

Samuelsson, J., Dawes, P. R. and Vidal, G., 1999, Organic-walled microfossils from the Proterozoic Thule Supergroup, northwestern Greenland: Precambrian Research, v. 96, p. 1–23.

Sergeev, V. N., 2001, Paleobiology of the Neoproterozoic (upper Riphean) Shorikha and Burovaya silicified microbiotas, Turukhansk Uplift, Siberia: Journal of Paleontology, v. 75, p. 427–448.

Sergeev, T. V., Knoll, A. H. and Petrov, P. Yu., 1997, Paleobiology of the Mesoproterozoic-Neoproterozoic transition: the Sukhaya Tunguska Formation, Turukhansk Uplift, Siberia: Precambrian Research, v. 85, p. 201-239.

Sergeev, V. N. and Lee Seong-Joo, 2006, Real eukaryotes and precipitates first found in the middle Riphean stratotype, southern Urals: Stratigraphy and Geological Correlation, v. 14, p. 1–18.

Sergeev, V. N. and Schopf, J. W., 2010, Taxonomy, paleoecology and biostratigraphy of the late Neoproterozoic Chichkan microbiota of south Kazakhstan: the marine biosphere on the eve of metazoan radiation: Journal of Paleontology, v. 84, p. 363–401.

Shaw, A. B., 1964, Time in Stratigraphy, McGraw-Hill, 365 pp.

Shen, S., Crowley, J.L., Wang, Y., Bowring, S.A., Erwin, D.H., Sadler, P.M., Cao, C., Rothman, D.H., Henderson, C.M., Ramezani, J., Zhan, H., Shen, Y., Wang, X., Wang, W., Mu, L., Li, W., Tang, Y., Liu, X., Liu, L., Zeng, Y., Jiang, Y., and Jin, Y., 2011, Calibrating the end-Permian mass extinction: Science, v.334, no.6061, p.1367-1372

Singh, V. K., Babu, R. and Shukla, M., 2009, Discovery of carbonaceous remains from the Neoproterozoic shales of Vindhyan Supergoup, India: Journal of Evolutionary Biology Research, v. 1, p. 1–17.

Simonetti, C. and Fairchild, T. R., 2000, Proterozoic microfossils from the subsurface siliciclastic rocks of the São Francisco Craton, south-central Brazil: Precambrian Research, v. 103, p. 1–29.

Srivastava, P., 2002, Carbonaceous megafossils from the Dholpura shale, uppermost Vindhyan Supergroup, Rajasthan: an age implication: Journal of the Palaeontological Society of India, v. 47, p. 97–105.

Srivastava, P., 2009, *Trachyhystrichosphaera*: an age-marker acanthomorph from the Bhander Group, upper Vindhyan, Rajasthan: Journal of Earth System Sciences, v. 118, p. 575–582.

Strauss, J., Rooney, A. D., Macdonald, F. A., Brandon, A. D and Knoll, A.H., 2014, 740 Ma vase-shaped microfossils from Yukon, Canada: Implications for Neoproterozoic chronology and biostratigraphy: Geology, v. 42, p. 659–662.

Sun, W., Wang, G. and Zhou, B., 1986, Macroscopic worm-like body fossils from the upper Precambrian (900–700 Ma), Huainan District, Anhui, China and their stratigraphic and evolutionary significance: Precambrian Research, v. 31, p. 377–403.

Swanson-Hysell, N. L., Maloof, A. C., Condon, D., J., Jenkin, G. R. T., Alene, M., Tremblay, M. M., Tesema, T., Rooney, A. D and Haileab, B., 2015, Stratigraphy and geochronology of the Tambien Group, Ethiopia: evidence for globally synchronous carbon isotope change in the Neoproterozoic: Geology, v. 43, p. 323–326.

Swanson-Hysell, N. L., Rose, C. V., Calmet, C. C., Halverson, G. P., Hurtgen, M. T. and Maloof, A. C., 2010, Cryogenian Glaciation and the onset of carbon-isotope decoupling: Science, v. 328, p. 608–611.

Tang, Q., Pang, K., Xiao, S., Yuan, X., Ou, Z. and Wan, B., 2013, Organic-walled microfossils from the early Neoproterozoic Liulaobei Formation in the Huainan region of North China and the biostratigraphic significance: Precambrian Research, v. 236, p. 157–181.

Tang, Q., Pang, K., Yuan, X., Wan, B. and Xiao, S., 2015, Organic-walled microfossils from the Tonian Gouhou Formation, Huaibei region, North China Craton, and their biostratigraphic implications: Precambrian Research, v. 266, p. 296–318.

Tripathy, G. R. and Singh, S. K., 2015, Re-Os depositional age for black shales from the Kaimur Group, Upper Vindhyan, India: Chemical Geology, v. 413, p. 63–72.

Van Acken, D., Thomson, D., Rainbird, R. H. and Creaser, R. A., 2013, Constraining the depositional history of the Neoproterozoic Shaler Supergroup, Amundsen Basin, NW Canada: Rhenium-osmium dating of black shales from the Wynniatt and Boot Inlet formations: Precambrian Research, v. 236, p. 124–131.

Veis, A. F., Petrov, P. U. and Vorob'eva, N. G., 1998, Miroedikha mikrobiota Verkhnego Rifeya Sibiri: Stratigrafiya. Geologicheskaya Korreliatsiya, v. 6, p. 15–37. (In Russian)

Vidal, G., 1976a, Late Precambrian microfossils from the Visingsö beds in Southern Sweden: Fossils and Strata, no. 9, p. 1–37.

Vidal, G., 1976b, Late Precambrian acritarchs from the Eleonore Bay Group and Tillite Group in East Greenland: Grønlands Geologiske Undersøgelse Rapport, no. 78, p. 1–19.

Vidal, G., 1979, Acritarchs from the upper Proterozoic and lower Cambrian of East Greenland: Grønlands Geologiske Undersøgelse Bulletin, no. 134, p. 1–40.

Vidal, G., 1981a, Aspects of problematic acid-resistant, organic-walled microfossils (acritarchs) in the upper Proterozoic of the North Atlantic region: Precambrian Research, v. 15, P. 9–23.

Vidal, G., 1981b, Micropaleontology and biostratigraphy of the Upper Proterozoic and Lower Cambrian sequence in East Finnmark, northern Norway: Norges Geologiske Undersøkelse, v. 362, p. 1–53.

Vidal, G. and Ford, T. D., 1985, Microbiotas from the Late Proterozoic Chuar Groups (Northern Arizona) and Uinta Mountain Group (Utah) and their chronostratigraphic implications: Precambrian Research, v. 28, p. 349–389.

Vidal, G. and Moczydłowska-Vidal, M., 1997, Biodiversity, speciation and extinction trends of Proterozoic and Cambrian phytoplankton: Paleobiology, v. 23, p. 230–246.

Vidal, G., Moczydłowska, M. and Rudavskaya, V. A., 1993, Biostratigraphic implications of a *Chuaria-Tawuia* assemblage and associated acritarchs from the Neoproterozoic of Yakutia: Palaeontology, v. 36, p. 387–402.

Vidal, G. and Siedlecka, A., 1983, Planktonic, acid-resistant microfossils from the upper Proterozoic strata of the Barents Sea region of Varanger Peninsula, east Finnmark, northern Norway: Norges Geologiske Undersøkelse, v. 382, p. 45–79.

Vorob'eva, N., Sergeev, V. N. and Knoll., A., 2009, Neoproterozoic microfossils from the northeastern margin of the East European Platform: Journal of Paleontology, v. 83, p. 161–196.

Wang, G., Zhang, S., Li, S., Yan, Y., Dou, S. and Fang, D., 1984, Research on the upper Precambrian of northern Jiangsu and Anhui provinces: Anhui Press of Science and Technology, Heifei, Anhui, 209 pp.

Willman, S., and Moczydłowska, M., 2008, Ediacaran acritarch biota from the Giles-1 drillhore, Officer Basin, Australia, and its potential for biostratigraphic correlation: Precambrian Research, v. 162, p. 498–530.

Xiao, S. and Dong, L., 2006, On the morphological and ecological history of Proterozoic macroalgae. *In* Xiao, S. and Kaufman, A.J. (Eds.), Neoproterozoic Geobiology and Paleobiology. Springer, Dordrecht, the Netherlands, pp. 57-90

Xiao, S., Knoll, A. H., Kaufman, A. J., Yin L. and Zhang Y., 1997, Neoproterozoic fossils in Mesoproterozoic rocks? Chemostratigraphic resolution of a biostratigraphic conundrum from the North China Platform: Precambrian Research, v. 84, p. 197–220.

Xiao, S., Shen, B., Tang, Q., Kaufman, A. J., Yuan, X., Li, J., and Qian, M., 2014, Biostratigraphic and chemostratigraphic constraints on the age of early Neoproterozoic carbonate successions in North China: Precambrian Research, v. 246, p. 208–225.

Xiao, S., Tang, Q., Hughes, N., McKenzie and R., Myrow, P., 2016, Biostratigraphic and detrital zircon age constraints on the basement of the Himalayan Foreland Basin: Implications for a Proterozoic link to the Lesser Himalaya and cratonic India, Terra Nova, v. 28, p. 419-426.

Yang, D-B., Xu, W-L., Xu, Y-G., Wang, Q-H., Pei, F-P., and Wang, F., 2012, U-Pb ages and Hf isotope data from detrital zircons in the Neoproterozoic sandstones f northen Jiangsu and southern Liaoning Provinces, China: implications for the late

Precambrian evolution of the southeastern North China Craton: Precambrian Research, v. 216–219, p. 162–176.

Ye, Q., Tong, J., Xiao, S., Zhu, S., An, Z., Tian, L. and Hu, J., 2015, The survival of benthic macroscopic phototrophs on a Neoproterozoic snowball Earth; Geology, v. 43, p. 507–510.

Yin, C., 1985, Micropalaeoflora from the late Precambrian in Huainan region of Anhui province and its stratigraphic significance: Professional papers of Stratigraphy and Palaeontology, v. 12, p. 97–119.

Yin, C., Liu, P., Awramik, S. M., Chen, S., Tang, F., Gao, L., Wang, Z. and Riedman, L. A., 2011, Acanthomorphic biostratigraphic succession of the Ediacaran Doushantuo Formation in the East Yangtze Gorges, South China: Acta Geologica Sinica, v. 85, p. 283–295.

Yin, L. and Sun, W., 1994, Microbiota from the Neoproterozoic Liulaobei Formation in the Huainan region, northern Anhui, China: Precambrian Research, v. 65, p. 95-114.

Yin, L., Zhu, M., Knoll, A. H., Yuan, X., Zhang, J. and Hu, J., 2007, Doushantuo embryos preserved inside diapause egg cysts: Nature, V. 446, p. 661–663.

Zang, W-L and Walter, M., 1992a, Late Proterozoic and Early Cambrian microfossils and biostratigraphy, northern Anhui and Jiangsu, central-eastern China: Precambrian Research, v. 57, p. 243–323.

Zang, W-L and Walter, M., 1992b, Late Proterozoic and Cambrian microfossils and biostratigraphy, Amadeus Basin, central Australia: Association of Australiasian Palaeontologists Memoir, no. 12, p. 1–132.

List of figures

Figure 1. Paleogeographic locations and table of sections. A paleogeographic reconstruction at ~780 Ma with red stars showing general locations of fossiliferous sections in database. Table records sections in database. See supplementary tables for further details. Craton/terrane abbreviations: A = Amazonia; Ae—Avalonia (east); Aw—Avalonia (west); B—Baltica; C—Congo; EA—East Antarctica; ES—East Svalbard; G—Greenland; I—India; K—Kalahari; L—Laurentia; NA—Northern Australia; NC—North China; R—Rio Plata; S—Sahara; SA—Southern Australia; SC—South China; Sf—Sao Francisco; Si—Siberia; T—Tarim; WA—West Africa. Modified from Li et al. 2013.

Figure 2. Ordinal, thickness-scaled and age-scaled species richness. Three stages in calibration of a taxon richness time series. (A) Cumulative running total of taxon richness calculated from CONOP placement of first and last occurrences in an ordinal best-fit sequence of events; each position in sequence is occupied by only one event; event spacing is uniform. (B) Thickness-scaled composite; spacing of adjacent events from (A) is scaled to their mean stratigraphic separation; sets of events whose internal sequence is not resolvable receive zero spacing. (C) Age-scaled composite; ages of events in (B) are estimated by piecewise linear interpolation. Bitter Springs and Islay carbon isotopic events and Sturtian and Marinoan glacial events are indicated throughout for temporal context. Grey buffer regions discussed in text section 2.4.2.

Figure 3. Age calibration of composite richness. Piecewise-linear age calibration curve for composite sequence (converts Fig. 2B to 2C). Red diamonds: coordinates of dated events in composite sequence and time scale (each event generates two symbols, e.g. the ends of a 2-sigma analytical uncertainty for radiometric dates or onset and termination of a glaciation.) Blue crosses: interpolated age for each event horizon in the interval-scaled composite. Grey buffer regions discussed in text section 2.4.2.

Figure 4. (A) Higher resolution 1Ga to 635 Ma age-scaled richness and (B) rarefied richness. (A) One representative richness solution (black line) shown against band (grey) encompassing the sum of five additional solutions. Variation results from heuristic approach of CONOP program combined with long-ranging or rare taxa that provide too little constraint for robust placement. (B) Rarefied richness curve (black line) of one richness solution in which data are reduced to a uniform sample size of 50 local ranges. Raw richness is unaltered in interval in which actual sample size was lower than 50 local ranges (dashed line). 95% confidence interval for rarefied solution (grey band). For both (A) and (B) note major features of record, i.e. richness increase onset ~800 Ma, peak ~775 to 770 Ma, broad decrease, sharp increase with appearance of VSM taxa, then decline with their loss and further drop into Islay carbon anomaly. Note scale changes to x-axis to show detail of interval of greatest activity. Grey buffer regions discussed in text section 2.4.2.

Figure 5. Taxon ranges for select taxa with compressed age-scaled richness. Estimated stratigraphic ranges for taxa that appear in four or more sections with no large gaps or outliers, and those suggested as index taxa. Numbers in parentheses next to taxa indicate number of sections in which they occur within the database. "VSM spp." Refers to all VSM taxa, including occurrences of specimens not resolvable to genus-level from published illustrations. "Eleven VSM species" indicates the stratigraphic ranges of the following species with occurrences in 1 to 5 sections within the database: *Bonniea dacruchares*, *B. pytinaia*, *Bombycion micron*, *Cycliocyrillium simplex*, *C. torquata*, *Hemisphaeriella ornata*, *Melanocyrillium hexodiadema*, *Melicerion poikilon*, *Palaeoarcella athanata*, *Trachycyrillium pudens*, *Trigonocyrillium horodyskii*. Note scale changes to x-axis. Grey buffer regions discussed in text section 2.4.2.

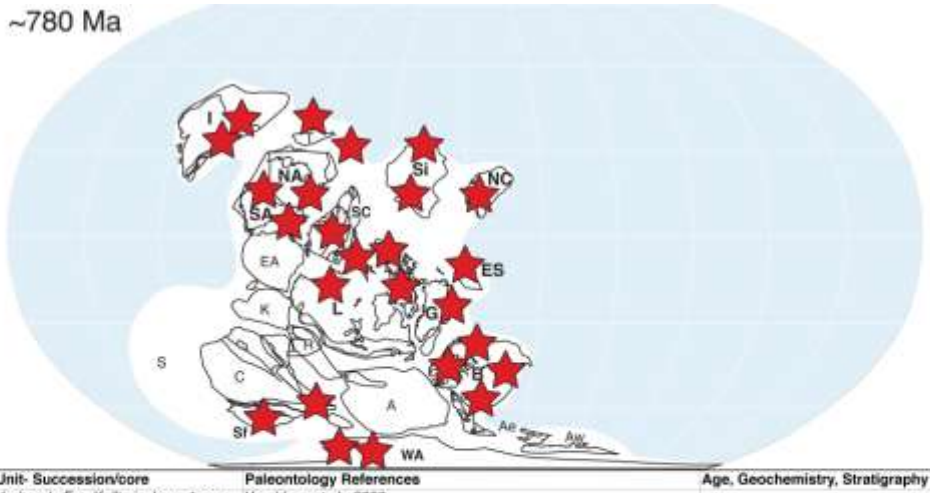

Paleocontinent	Unit- Succession/core	Paleontology References	Age, Geochemistry, Stratigraphy References
Baltica	Vychegda Fm- Kel'tminskaya-1 core	Vorob'eva et al., 2009	
Baltica	Karatau Group	Nyberg and Schopf, 1984	Sergeev and Lee, 2006
Baltica	Yurmata Group	Jankauskas, 1978; 1979; Sergeev and Lee, 2006	
Baltica	Maly Karoy Group	Sergeev and Schopf, 2010	Levashova et al., 2011
Baltica	Vadsø, Tanafjord and Smalfjord grps	Vidal, 1981	
Baltica	Chaporna Fm- Kola Peninsula	Samuelsson, 1997	
Baltica	Kildinskaya Group	Samuelsson, 1997	
Baltica	Barents Sea Group	Vidal and Siedlecka, 1983	
Baltica	Visingsö Group	Vidal, 1976a, Marti Mus and Moczydłowska, 2000, Porter et al., 2003	Moczydłowska et al., 2017
Greenland+ Svalbard	Eleonore Bay + Tillite groups	Vidal, 1976b; Vidal, 1979	
Greenland+ Svalbard	Thule Supergroup	Samuelsson et al., 1999	
Greenland+ Svalbard	Veteranen+ Akademikerbreen+ Polarisbreen groups	Knoll and Swett, 1985; Knoll et al., 1989; Knoll et al., 1991; Butterfield et al., 1994; Butterfield, 2004; Riedman et al., 2014; LAR pers. obs.	Halverson et al., 2007; Hoffmann et al., 2012
Greenland+ Svalbard	Roaldtoppen Group	Knoll and Calder,1983; Knoll, 1984	
N. China	Huaibei Group	Wang et al., 1984; Zang and Walter, 1992a; Dong et al., 2008; Qian et al., 2009; Xiao et al., 2014, Tang et al 2015	Yang et al., 2012; Xiao et al., 2014
N. China	Huainan+Feishui groups	Wang et al., 1984; Yin, 1985; Sun et al., 1986; Zang and Walter, 1992a; Yin and Sun, 1994; Hong et al., 2004; Dong et al., 2008; Qian et al., 2009; Tang et al, 2013	Xiao et al., 2014
N. China	Qingbaikou System	Du and Tian, 1985	
South China	Nantuo Formation	Ye et al., 2015	Condon et al., 2005; McFadden et al., 2009
Altaids	Tayhr Fm- Tsagaan Oloom Group	Bosak et al., 2011a, b; Cohen et al., 2015	Macdonald et al., 2009; Bold et al., 2016
Siberia	Turukhansk Uplift	Petrov and Veis, 1995; Sergeev et al, 1997; Veis et al., 1998; Sergeev, 2001	
Siberia	Olenek Uplift	Vidal et al., 1993	
N. Laurentia	Fifteenmile Group	Allison and Hilgert, 1986; Allison and Awramik, 1989; Cohen and Knoll, 2012	Macdonald et al., 2010; Cohen et al.,2017
N. Laurentia	Bylot Supergroup	Hofmann and Jackson, 1994; Knoll et al., 2013	Heaman, 1992; Gibson, in prep
N. Laurentia	Mount Harper Group	Strauss et al., 2014	Macdonald et al., 2010; 2011; Rooney et al., 2014; 2015
N. Laurentia	Chuar Group	Vidal and Ford, 1985; Porter et al., 2003; Porter and Riedman, 2016	Karlstrom et al., 2000; Dehler et al., 2014; Rooney et al., in press
N. Laurentia	Little Dal Group	Hofmann and Aitken, 1979; Hofmann, 1985	Macdonald et al., 2010; Rooney et al., 2014; 2015
N. Laurentia	Blackwater Lake G-52 core	Samuelsson and Butterfield, 2001	
N. Laurentia	Loneland Fm- Franklin Mts	Samuelsson and Butterfield, 2001	
N. Laurentia	Uinta Group	Vidal and Ford, 1985, Nagy et al., 2005	Dehler et al., 2007
N. Laurentia	Shaler Supergroup	Hofmann and Rainbird, 1995; Butterfield, 2005a, 2005b	Jones et al., 2010; Macdonald et al., 2010; Van Acken et al., 2013
South Australia	Alinya Formation, Officer Basin	Willman and Moczydłowska, 2008; Riedman and Porter, 2016	
South Australia	Buldya Group, Officer Basin	Cotter, 1997; Cotter, 1999; Grey, 1999; Grey et al., 2011	
South Australia	Umberatana Group	Grey et al., 2003; Riedman et al., 2014	Kendall et al., 2006
South Australia	Togari Group	Riedman et al., 2014	Kendall et al., 2009; Calver, 2011
North Australia	Bitter Springs, Areyonga, Aralka fms	Zang and Walter, 1992b; Grey et al., 2003; Riedman et al., 2014	Kendall et al., 2006; Ambrose et al., 2010; Swanson-Hysell et al., 2010
India	Vindhyan Supergroup	Prasad et al., 2005; Srivastava, 2002, 2009; Singh et al., 2009	Tripathy and Singh, 2015
India	Ganga Supergroup	Xiao et al., 2016	McKenzie et al., 2011
West Africa	Kwahu, Oti/Pendjari groups, Ghana	Amard, 1984; Amard and Affaton, 1984; Coulffé and Vecoli, 2011	
West Africa	Atar/El Mreïti Group, Mauritania	Beghin et al., 2017	Rooney et al., 2010
Congo	Rasthof Fm, Otavi Group	Bosak et al., 2011; 2012; Dalton et al., 2012	
Congo-São Francisco	Mbuji-Mayi Sprgp, Dem. Rep. of Congo	Baludikay et al., 2016	Cahen et al., 1984; François et al., 2015; 2016
São Francisco	Bambuí + Conselheiro grps, Brazil	Simonetti and Fairchild, 2000	

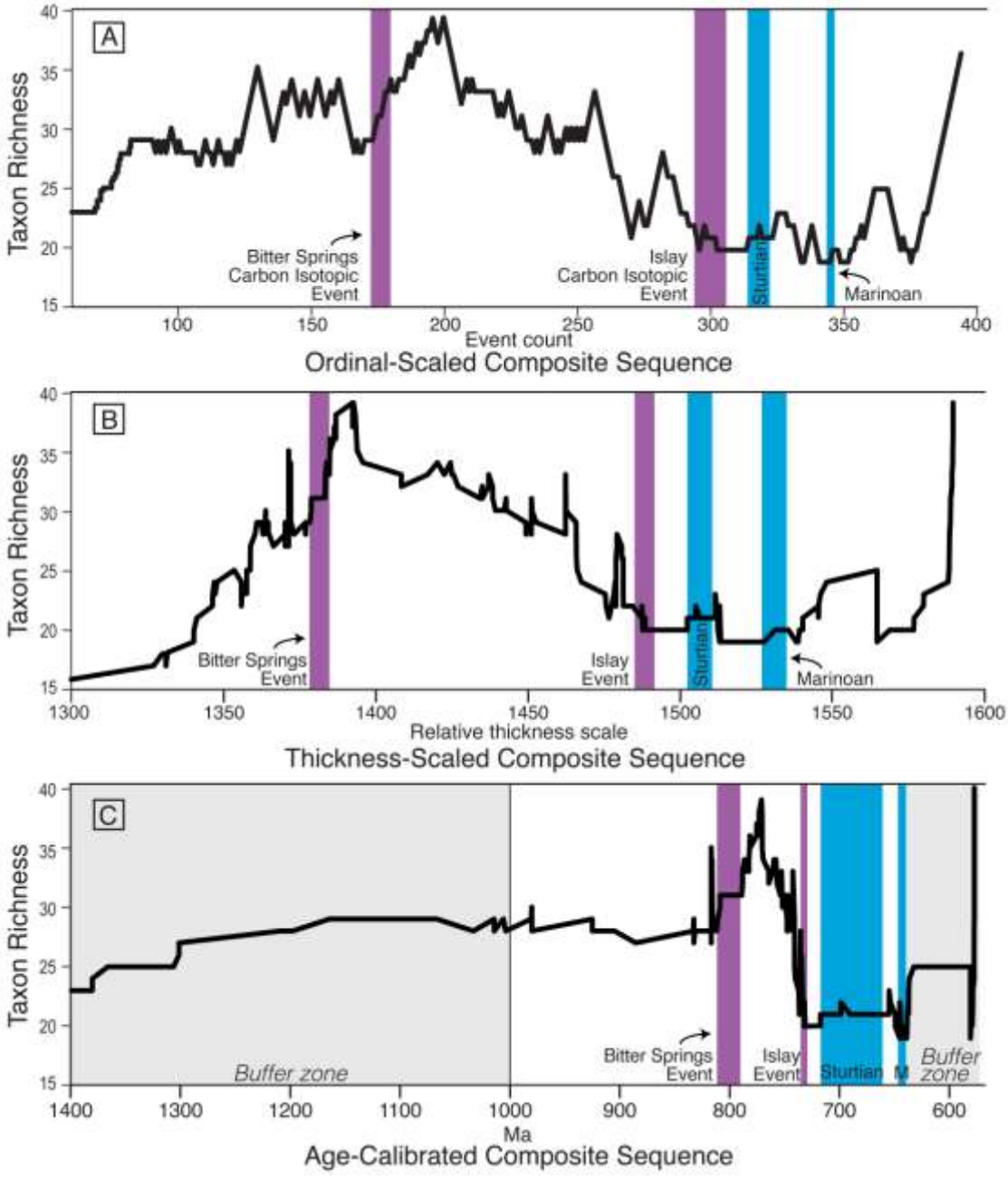
A
Taxon Richness
Bitter Springs Carbon Isotopic Event
Islay Carbon Isotopic Event
Sturtian
Marinoan
Event count
Ordinal-Scaled Composite Sequence
B
Taxon Richness
Bitter Springs Event
Islay Event
Sturtian
Marinoan
Relative thickness scale
Thickness-Scaled Composite Sequence
C
Taxon Richness
Buffer zone
Bitter Springs Event
Islay Event
Sturtian
M
Buffer zone
Ma
Age-Calibrated Composite Sequence

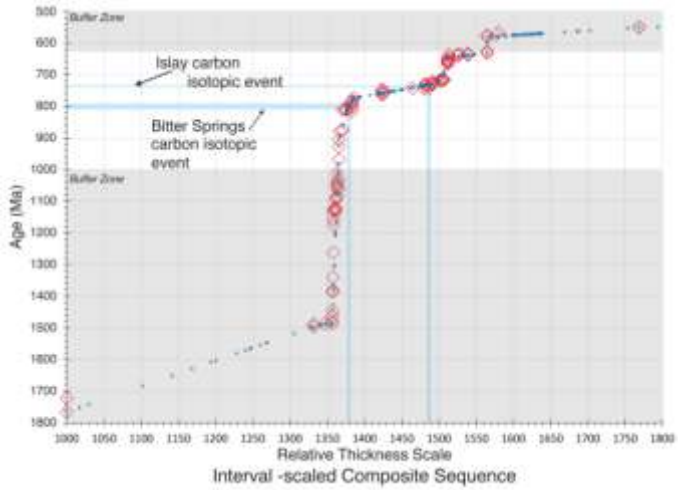

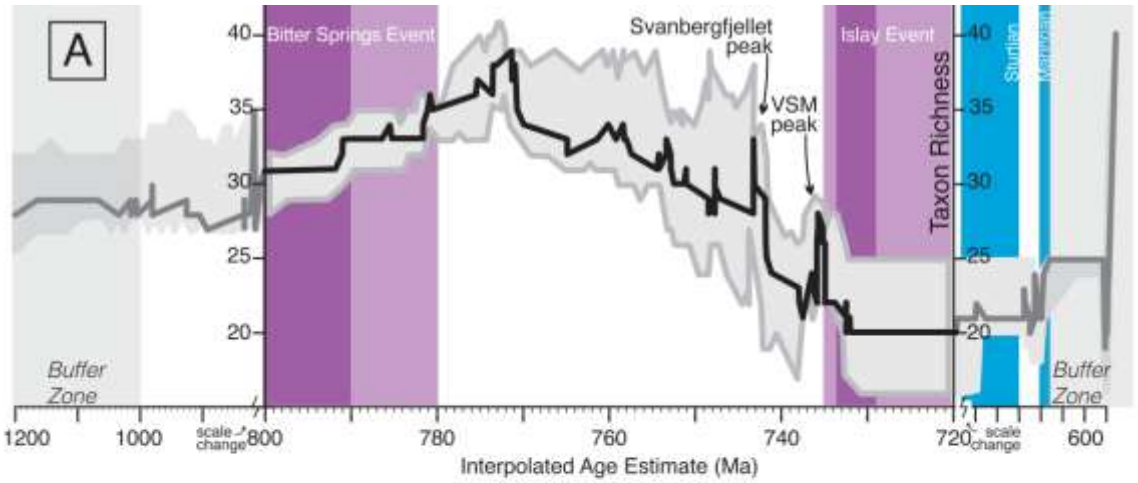
A
Bitter Springs Event
Svanbergfjellet peak
VSM peak
Islay Event
Taxon Richness
Buffer Zone
Buffer Zone
scale change
scale change
1200
1000
800
780
760
740
720
600
Interpolated Age Estimate (Ma)

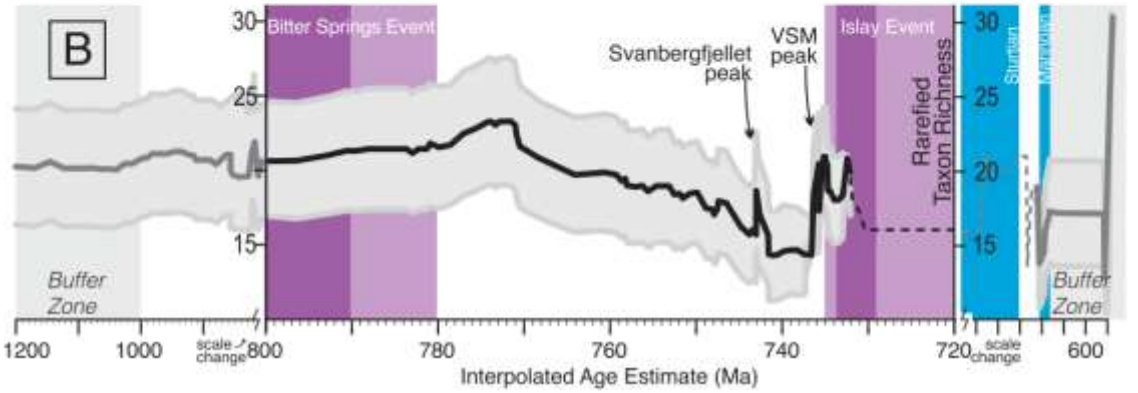
B
Bitter Springs Event
Svanbergfjellet peak
VSM peak
Islay Event
Rarefied Taxon Richness
Buffer Zone
Buffer Zone
scale change
scale change
1200
1000
800
780
760
740
720
600
Interpolated Age Estimate (Ma)

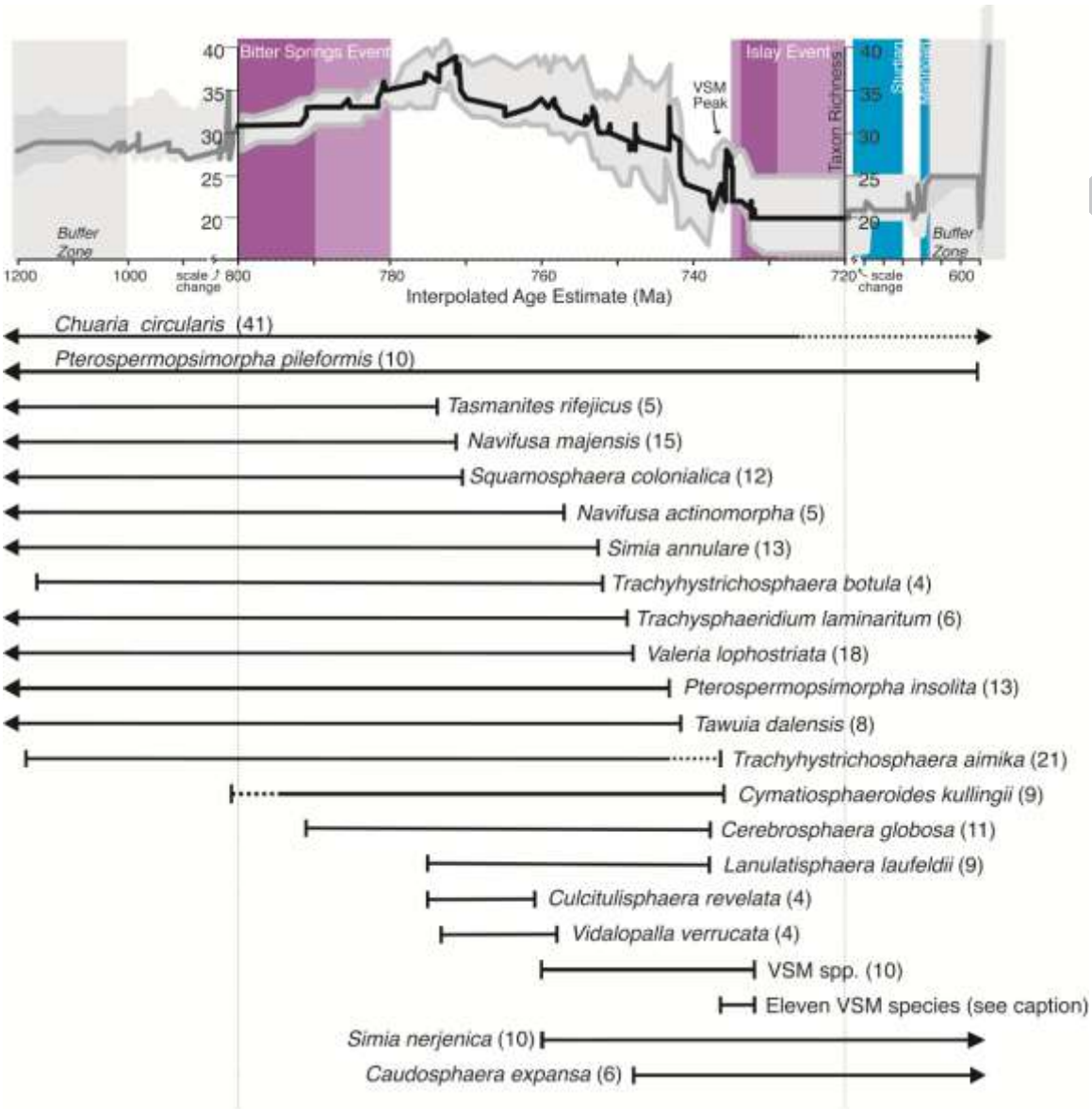
Bitter Springs Event
Islay Event
VSM Peak
Taxon Richness
Sturtian
Marinoan
Buffer Zone
Buffer Zone
scale change
scale change
Interpolated Age Estimate (Ma)
Chuaria circularis (41)
Pterospermopsimorpha pileformis (10)
Tasmanites rifejicus (5)
Navifusa majensis (15)
Squamosphaera colonialica (12)
Navifusa actinomorpha (5)
Simia annulare (13)
Trachyhystrichosphaera botula (4)
Trachysphaeridium laminaritum (6)
Valeria lophostriata (18)
Pterospermopsimorpha insolita (13)
Tawuia dalensis (8)
Trachyhystrichosphaera aimika (21)
Cymatiosphaeroides kullingii (9)
Cerebrosphaera globosa (11)
Lanulatisphaera laufeldii (9)
Culcitulisphaera revelata (4)
Vidalopalla verrucata (4)
VSM spp. (10)
Eleven VSM species (see caption)
Simia nerjenica (10)
Caudosphaera expansa (6)

Highlights for "Global species richness record and biostratigraphic potential of early to middle Neoproterozoic eukaryote fossils" Leigh Anne Riedman and Peter Sadler

- Use CONOP program to estimate eukaryotic species richness for Tonian and Cryogenian
- Richness peak ~770Ma, decline of acritarchs, brief pulse of VSM taxa, further drop
- Richness declines, many extinctions occur well before Snowball Earth glaciations
- We assess index taxa, find support for *Cerebrosphaera globosa* and species of VSMs